

Copyright © 1968, by the author(s).  
All rights reserved.

Permission to make digital or hard copies of all or part of this work for personal or classroom use is granted without fee provided that copies are not made or distributed for profit or commercial advantage and that copies bear this notice and the full citation on the first page. To copy otherwise, to republish, to post on servers or to redistribute to lists, requires prior specific permission.

COMPUTER STUDIES OF TEMPERATURE COMPENSATION  
IN SELECTIVE AMPLIFIERS

by

William J. McCalla

Memorandum No. ERL-M 250

27 June 1968

ELECTRONICS RESEARCH LABORATORY

College of Engineering  
University of California, Berkeley  
94720

## ACKNOWLEDGMENT

The author is indebted to Professor D. O. Pederson for the guidance and support provided during the preparation of this report. Also the author wishes to acknowledge the many helpful conversations with Messrs. P. L. Lee and B. A. Wooley.

Research sponsored by the U. S. Army Research Office--  
Durham under Contract DAHCO4-67-C 0031.

## TABLE OF CONTENTS

	page
INTRODUCTION	1
I. FIRST-ORDER TEMPERATURE SENSITIVITY IN MONOLITHIC SELECTIVE AMPLIFIERS	3
A. Introduction to Feedback in Active RC Selective Amplifiers	3
B. Sensitivity Functions in Single-Loop Feedback Amplifiers	13
C. Low-Frequency Temperature Dependence in Monolithic Integrated Circuits	21
D. Partially Compensated Selective Amplifier	37
II. COMPENSATION WITH ADDITIONAL DEGREES OF FREEDOM	51
III. THE TEMPERATURE COMPENSATED SELECTIVE AMPLIFIER	62
SUMMARY	106
REFERENCES	109
APPENDIX A: SENSITIVITY OF CLOSED-LOOP POLES IN SINGLE-LOOP FEEDBACK	111

## INTRODUCTION

Of particular importance in the realization of selective amplifiers is the sensitivity of the response to both active and passive components where response invariance can be characterized by constant center frequency and constant bandwidth. Active RC selective amplifier designs are commonly based on gyrator,<sup>1,2</sup> negative impedance converter,<sup>3-5</sup> positive immittance inverter,<sup>6</sup> or feedback amplifier realizations. In previous work, Gaash developed three temperature insensitive selective amplifier design procedures based on first-order considerations.<sup>7,8</sup> In this report this work is re-examined and extended for the single-loop configuration. Emphasis is placed on designs compatible with the limitations imposed by present levels of monolithic diffused integrated circuit technology.

The procedure and typical realization proposed by Gaash are studied with respect to a range of values of temperature coefficients of circuit and device parameters. Effects of charge storage (excess phase) in active devices and due to parasitics are considered. Losses brought in by second-order models of active devices are examined. Problems due to tolerance effects and imperfect integrated realization are considered. For this work, extensive computer-aided analysis is used. This includes simulation and temperature analysis with several standard circuit

analysis programs.<sup>9-11</sup> As the design procedure proposed by Gaash was graphical in nature, root locus techniques are used extensively.

I. FIRST-ORDER TEMPERATURE SENSITIVITY  
IN MONOLITHIC SELECTIVE AMPLIFIERS

A. INTRODUCTION TO FEEDBACK IN ACTIVE RC SELECTIVE AMPLIFIERS

Feedback amplifiers provide a convenient way to realize a dominant complex pair of natural frequencies necessary for active RC selective amplifiers. The general form of the feedback equation is

$$A(s) = \frac{a(s)}{1 - a(s)f(s)} \quad (1)$$

$$= \frac{a(s)}{1 + T(s)} \quad (2)$$

where

$A(s)$  = closed-loop transfer function

$a(s)$  = forward transmission function

$f(s)$  = feedback function

$T(s)$  = loop transmission function

The natural frequencies of the amplifier which are the poles of  $A(s)$  are given by the zeros of  $1 + T(s)$ , the return difference. To illustrate the dependence of natural frequencies on the feedback function, consider the following example where the forward transmission function is given by

$$a(s) = \frac{a(0)}{(1 - s/p_1)(1 - s/p_2)} = \frac{a(0)b_0}{s^2 + b_1s + b_0} \quad (3)$$

and the feedback function is given by

$$f(s) = f(0) \quad (4)$$

and is assumed to be constant with respect to frequency.

The closed-loop transfer function can be expressed as

$$A(s) = \frac{a(0)b_0}{s^2 + b_1s + b_0(1 + T_0)} \quad (5)$$

where  $T_0$  is defined by

$$T_0 = T(0) = -a(0)f(0) \quad (6)$$

As  $f(0)$  is varied from zero to infinity, the poles of  $A(s)$  move away from  $p_1$  and  $p_2$ , the poles of  $a(s)$ , as shown in Fig. 1. The loci of the poles  $A(s)$  can be constructed with familiar root-locus techniques.<sup>12</sup>

By way of further illustration, consider the shunt-series feedback pair of Fig. 2. Resistor values shown were chosen to achieve the approximate bias currents indicated while satisfying the constraints imposed by requirements on  $T_0$  as will be pointed out shortly.  $C_1$  and  $C_2$  are to be chosen such that the closed-loop response has a center frequency  $\omega_0 = 10^6$  rad/sec and a selectivity, or ratio of center frequency to bandwidth,  $Q \geq 10$ . For these values a narrowband situation exists; the center frequency, bandwidth, and selectivity can be expressed in terms of the dominant pair of natural frequencies  $q_{1,2} = \sigma_1 \pm j\omega_1$ .



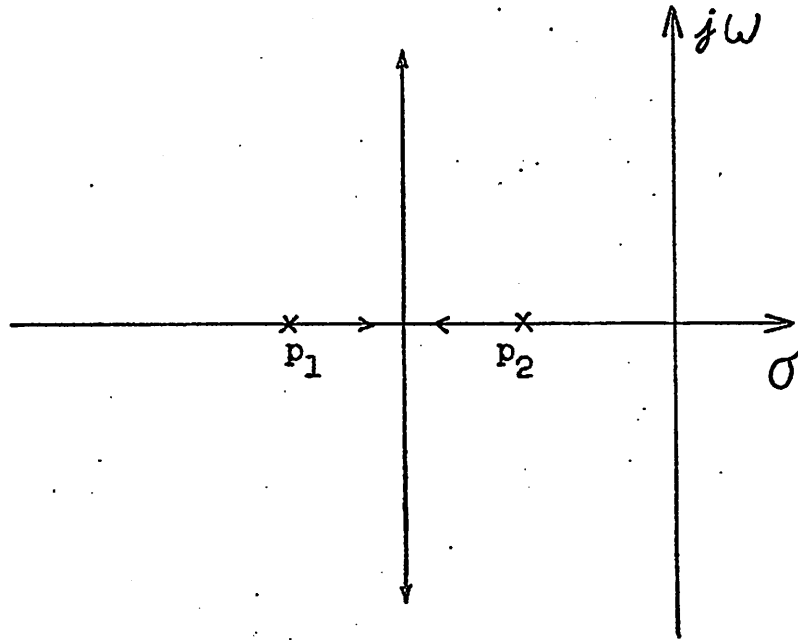
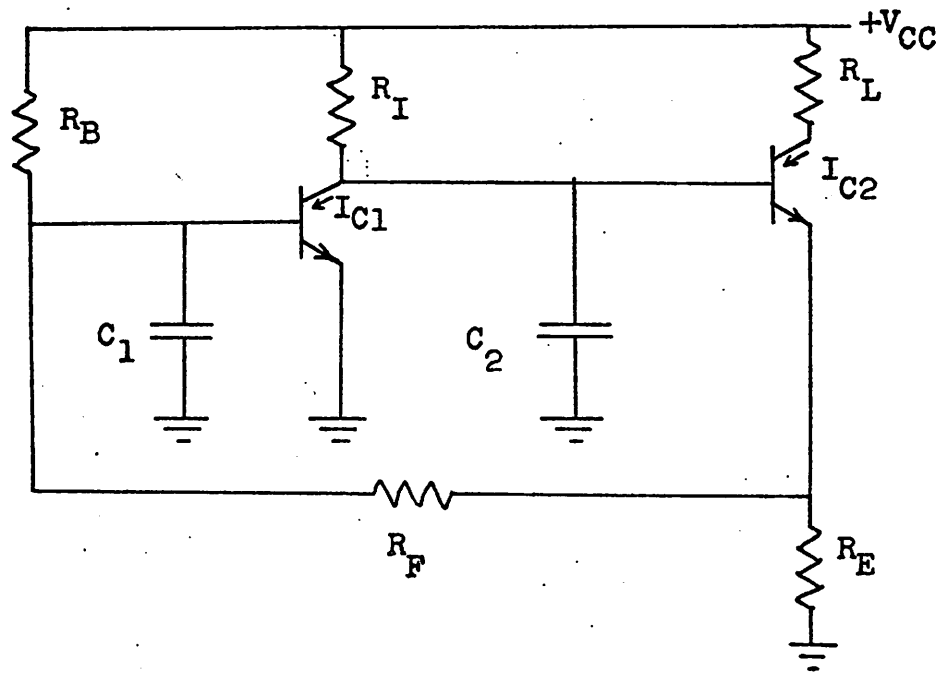


Fig. 1. Root locus.



$$\begin{aligned}
 V_{CC} &= 6.5 \text{ V} & R_B &= 13 \text{ k}\Omega \\
 R_I &= 2.6 \text{ k}\Omega & R_L &= 3 \text{ k}\Omega \\
 R_F &= 90 \Omega & R_E &= 270 \Omega \\
 I_{C1} &= I_{C2} & &= 2 \text{ mA}
 \end{aligned}$$

Fig. 2. Shunt-series feedback pair.

$$\omega_0 \approx \omega_1 \quad BW \approx -2\sigma_1 \quad Q \approx -\omega_1/2\sigma_1 \quad (7)$$

A first-order, small-signal representation of the shunt-series feedback pair is presented in Fig. 3. The feedback loop has been broken so as to be able to characterize the forward transmission function and the feedback function in terms of the circuit elements and parameters. A discussion of this method of obtaining the open-loop response and the assumptions upon which this method is based is presented in SEEC, Vol. V.<sup>13</sup> Note that the low-frequency, first-order approximation, as shown in Fig. 4(b), to the hybrid-pi transistor model of Fig. 4(a) has been used in the representation of Fig. 3(a).<sup>#</sup>

The forward current gain function is given by

$$a_I(s) = \frac{I_L'}{I_S} = \frac{a_I(0)}{(1 - s/p_1)(1 - s/p_2)}$$

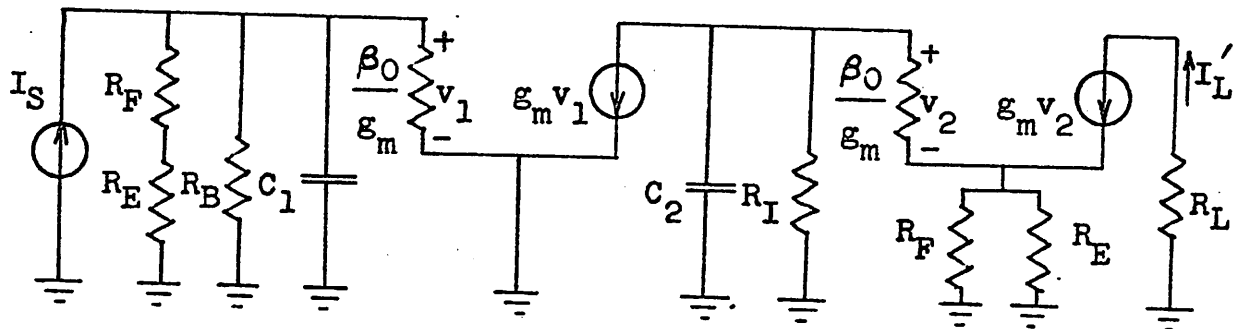
where from Fig. 3(a)

$$a_I(0) = \frac{-\beta_0 R_B \parallel (R_F + R_E)}{R_B \parallel (R_F + R_E) + \beta_0 / g_m} \cdot \frac{\beta_0 R_I}{R_I + \beta_0 / g_m + (\beta_0 + 1) R_F \parallel R_E}$$

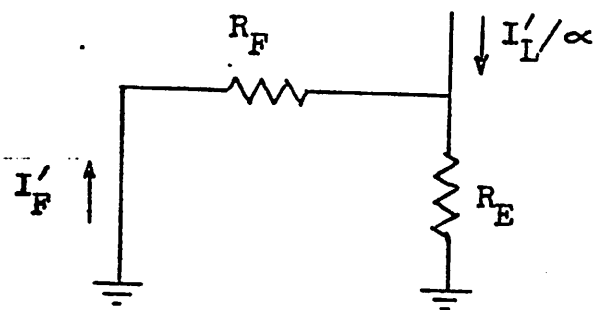
$$p_1 = -1/R_1 C_1$$

---

<sup>#</sup> A more complete discussion of the hybrid-pi model of Fig. 4(a) is presented in Section I.C when the sensitivity of the elements and parameters with respect to temperature is considered.

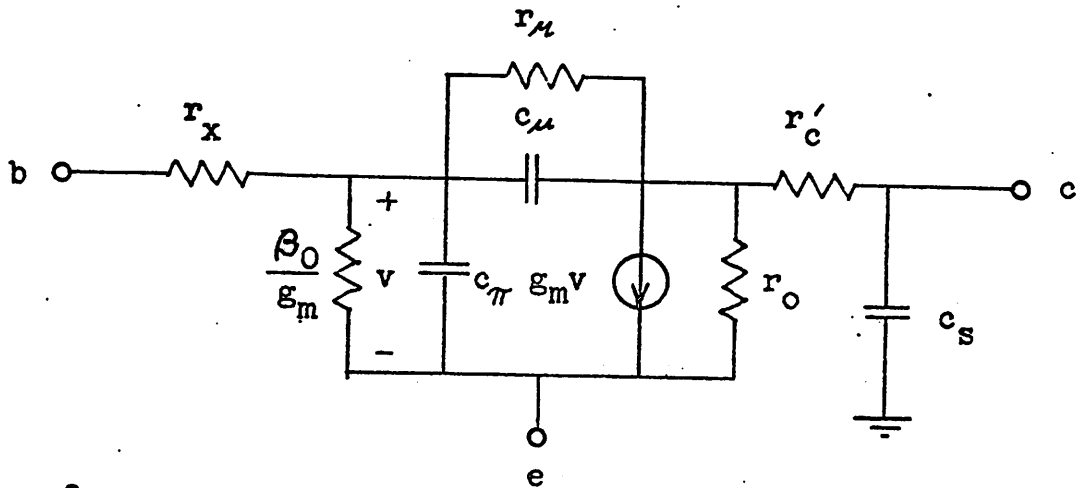


(a)



(b)

Fig. 3. (a) Forward transmission and (b) feedback networks.



$$\beta_0 = 100$$

$$f_t = 600 \text{ MHz.}$$

$$c_\pi = g_m / 2\pi f_t - c_\mu$$

$$c_\mu = 1 \text{ pF.}$$

$$c_s = 2 \text{ pF.}$$

$$g_m = qI_C / kT \text{ } \Omega^{-1}$$

$$r_x = 100 \text{ } \Omega$$

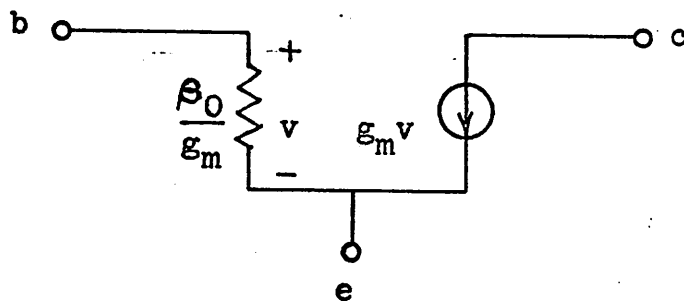
$$r_\mu = 5 \text{ M}\Omega$$

$$r_o = 50 \text{ k}\Omega$$

$$r'_c = 50 \text{ } \Omega$$

$$T = 300^\circ \text{K}$$

(a)



$$\beta_0 = 100$$

$$g_m = qI_C / kT$$

(b)

Fig. 4. (a) Hybrid-pi transistor model with typical parameter values. (b) First-order approximation to hybrid-pi model.

$$p_2 = -1/R_2 C_2$$

and the equivalent resistances  $R_1$  and  $R_2$  are given by

$$R_1 = R_B \parallel [(R_F + R_E) \parallel \beta_o / \beta_m]$$

$$R_2 = R_I \parallel [\beta_o / \beta_m + (\beta_o + 1) R_F \parallel R_E]$$

The feedback function is given by

$$f_I(s) = \frac{I'_F}{I'_L / \alpha}$$

which from Fig. 3(b) can be written

$$f_I(s) = f_I(0) = \frac{I'_F}{I'_L} = - \frac{\alpha R_E}{R_F + R_E} \approx \frac{-R_E}{R_F + R_E}$$

where  $\alpha$ , the common-base, short-circuit current gain, is assumed to be approximately one. The closed-loop current gain can be written

$$A_I(s) = \frac{a_I(0) / R_1 R_2 C_1 C_2}{s^2 + (1/R_1 C_1 + 1/R_2 C_2) s + (1 + T_0) / R_1 R_2 C_1 C_2}$$

Assume for convenience that the two open-loop poles  $p_1$  and  $p_2$  are equal

$$p_1 = p_2 = p$$

The closed-loop current gain may then be expressed by

$$-A_I(s) = \frac{a_I(0)p^2}{s^2 - 2ps + p^2(1 + T_0)}$$

and the poles of  $A_I(s)$  are given by

$$a_{1,2} = \sigma_1 \pm j\omega_1 = p \mp jp\sqrt{T_0}$$

The center frequency, bandwidth, and selectivity are

$$\omega_0 \approx -p\sqrt{T_0} \quad BW \approx -2p \quad Q \approx \sqrt{T_0}/2$$

Based on the required value of center frequency,  $\omega_0$ , and the assumed element values,  $C_1$  and  $C_2$  are found to be 0.075  $\mu$ F and 0.011  $\mu$ F, respectively, where from the expressions given above,  $R_1 \approx 272 \Omega$ ,  $R_2 \approx 1.97 \text{ k}\Omega$ , and  $T_0 \approx 400$ . These results are summarized and presented below in the first column of Table 1. The second column presents the results of a computer analysis of the circuit representations of Fig. 3 and of the closed-loop response.<sup>#</sup> The third column presents the results of a computer analysis of the circuits of Fig. 3 and of the closed-loop response where the hybrid-pi model of Fig. 4(a) has been used instead of the first-order model of Fig. 4(b). Consider the results of the first-order analysis. The noticeable shift in the real part of the closed-loop poles is explained by the presence of a

<sup>#</sup> Throughout this report, analyses in which the reduced hybrid-pi model of Fig. 4(b) are used will be referred to as first-order, while those in which the hybrid-pi model of Fig. 4(a) are used will be referred to as second-order.

Table 1

Results from Shunt-Series Feedback Pair  
(Frequency in rad/sec x 10<sup>6</sup>)

	Design	First-Order	Second-Order
$a_I(0)$	-534	-540	-460
$f_I(0)$	0.75	0.75	0.75
$T_I(0)$	400	405	346
$p_1$	-0.0500	-0.0458	-0.0483 + j0.0035
$p_2$	-0.0500	-0.0487	-0.0483 - j0.0035
$q_{1,2}$	-0.0500 ± j1.00	-0.0942 ± j0.948	-0.0915 ± j0.899
$\omega_o$	1.00	0.948	0.899
BW	0.100	0.188	0.183
Q	10.0	5.0	4.9



transmission zero on the negative real axis at  $-9.13 \times 10^6$  rad/sec. This zero results from forward transmission through the feedback network and could be eliminated by applying the signal at the collector of the first transistor. From the results of the second-order analysis, it can be seen that losses due to loading by  $r_x$ ,  $r_\mu$ ,  $r_o$ , and  $r_c'$  have reduced the low-frequency value of the loop transmission,  $T_0$ .

To conclude, feedback amplifiers can be used to realize a dominant complex pair of natural frequencies, although first-order design procedures can, at best, only approximate the desired results. Excess phase and interaction effects due to charge storage and the finite loads introduced by actual transistors must be treated in the final design, or else designs must be used which sufficiently minimize these effects.

#### B. SENSITIVITY FUNCTIONS IN SINGLE-LOOP FEEDBACK AMPLIFIERS

It is to be expected that variations in the characteristics of passive and active components with respect to temperature will produce corresponding variations in the open-loop singularities and in the low-frequency value of the loop transmission,  $T_0$ . Since the root locus is a function of the entire configuration of open-loop poles and zeros, the net effect of any variation in the open-loop poles or zeros is to change the shape of the root locus; similarly, variations in  $T_0$  produce changes in the positions

on the loci of the closed-loop poles. Thus it can be concluded that the closed-loop poles will suffer some displacement as temperature changes. A crucial observation is that for small increments, it is possible to reduce the net displacement in any closed-loop pole into two components--one component to represent the motion of a pole along a particular locus as a function of variations in  $T_0$  and a second component to represent the variation in a pole location due to the change in shape of the particular locus considered.

The use of monolithic integrated circuits allows one to take advantage of the inherent homogeneity of elements of the same type. By requiring that all dominant open-loop singularities be determined by passive RC products, Gaash obtained a simple expression for the second component to pole displacement mentioned above. It should be noted, however, that the use of monolithic diffused integrated circuits places limitations on the range of values which passive diffused resistors may assume.

It is apparent that a more detailed analysis of the effects of temperature on gain parameters and network function singularities is required. It is convenient to introduce two sensitivity functions. Root sensitivity, introduced by Horowitz<sup>14</sup>, expresses the sensitivity of a singularity with respect to a parameter  $x$  and is defined according to

$$-\frac{S^{q_1}}{x} = \frac{\partial q_1}{\partial x/x} = x \frac{\partial q_1}{\partial x} \quad (8)$$

This is the ratio of the variation in the singularity  $q_1$  to the fractional change in the sensitive parameter  $x$ . In this manner the phase of  $S_x^{q_1}$  is identified with the phase of the incremental displacement of the singularity,  $dq_1$ . Classical sensitivity as defined by Bode<sup>15</sup> and later modified by Mason<sup>16</sup> is a first-order sensitivity function defined according to

$$\frac{S^F}{x} = \frac{\partial F/F}{\partial x/x} = x \frac{\partial \ln F}{\partial x} = \frac{\partial \ln F}{\partial \ln x} \quad (9)$$

This is the ratio of the fractional change in the value of the function  $F$  to the fractional change in the sensitive parameter  $x$ . Note that in general, root sensitivity has a phase associated with it, whereas classical sensitivity has an associated phase when  $F$  is complex but none when  $F$  is scalar.

These two sensitivity functions may be used to relate changes in amplifier response to changes in sensitive parameters. Assume that the closed-loop transfer function,  $A(s)$ , of a single-loop feedback amplifier is written in the form

$$A(s) = \frac{N(s)}{D(s)} = \frac{N(s)}{1 + T(s)} \quad (10)$$

where  $D(s)$  (not necessarily a polynomial) is the return difference and  $T(s)$  is the loop transmission function.  $T(s)$  may be written in one of the two forms<sup>#</sup>

$$T(s) = T_0 \frac{\prod_k (1 - s/z_k)}{\prod_e (1 - s/p_e)} \quad (11)$$

$$= K \frac{\prod_k (s - z_k)}{\prod_e (s - p_e)} \quad (12)$$

where the low-frequency value of the loop transmission,  $T_0$ , is given by

$$T_0 = T(0) \quad (13)$$

---

<sup>#</sup> The symbol,  $z_k$ , will be used to denote any of the set of open-loop zeros  $z_1, z_2, \dots, z_m$ ; similarly, the symbol,  $p_e$ , to denote the set of open-loop poles  $p_1, p_2, \dots, p_n$ ; and the symbol,  $q_i$ , to denote the set of closed-loop poles  $q_1, q_2, \dots, q_n$ , where a proper system ( $n \geq m$ ) is assumed. In the absence of more specific notation,  $\prod_k$  will be used to indicate a product over the range of the index  $k$  ( $=1, 2, \dots, m$ ), and  $\prod_e$  and  $\prod_i$ , to indicate products over the respective ranges of the indices  $e$  ( $=1, 2, \dots, n$ ) and  $i$  ( $=1, 2, \dots, n$ ). Analogously, the notation  $\sum_k$ ,  $\sum_e$ , and  $\sum_i$  will be used to indicate a summation over the respective ranges of the indices  $k$ ,  $e$ , and  $i$ .

and where  $K$  is defined by

$$K = T(0) \frac{\prod_e (-p_e)}{\prod_k (-z_k)} \quad (14)$$

Let  $q_i$  denote a pole of  $A(s)$ , i.e. a zero of the return difference,  $D(s)$ . Under these assumptions, the following relations, developed in Appendix A of this report and alternatively by Kuh and Rohrer<sup>17</sup>, can be shown to hold

$$dq_i = S_{T_0}^{q_i} \frac{dT_0}{T_0} + S_{T_0}^{q_i} \sum_e \frac{q_i}{q_i - p_e} \frac{dp_e}{p_e} - S_{T_0}^{q_i} \sum_k \frac{q_i}{q_i - z_k} \frac{dz_k}{z_k} \quad (15)$$

$$S_{T_0}^{q_i} = \text{Res} \frac{\prod_e (s - p_e)}{\prod_j (s - q_j)} \Big|_{s=q_i} = \frac{\prod_e (s - p_e)}{\frac{\partial}{\partial s} \prod_j (s - q_j)} \Big|_{s=q_i} \quad (16)$$

$$= \left( \sum_e \frac{1}{s - p_e} - \sum_k \frac{1}{s - z_k} \right) \Big|_{s=q_i}^{-1} \quad (17)$$

Eq. 15 relates the incremental change in the closed-loop pole  $q_i$  to fractional changes in the low-frequency value of the loop transmission and the open-loop poles and zeros. Eqs. 16 and 17 give two expressions for the sensitivity of the closed-loop pole  $q_i$  with respect to  $T_0$ . Note that the evaluation of the second expression requires only a knowledge of the open-loop poles and zeros.

Consider a singularity  $r_j$  ( $= p_e$  or  $z_k$ ) of a feedback amplifier under open-loop conditions which is determined by the

product of the passive elements  $R_j$  and  $C_j$  both of which are assumed to be sensitive functions of temperature

$$r_j = \frac{1}{R_j C_j} \quad (18)$$

where

$$\begin{aligned} R_j &= R_j(T) \\ C_j &= C_j(T) \end{aligned} \quad (19)$$

Taking the total differential with respect to temperature, one obtains

$$\begin{aligned} dr_j &= \frac{\partial r_j}{\partial R_j} \frac{\partial R_j}{\partial T} dT + \frac{\partial r_j}{\partial C_j} \frac{\partial C_j}{\partial T} dT \\ &= -r_j \left( \frac{1}{R_j} \frac{\partial R_j}{\partial T} + \frac{1}{C_j} \frac{\partial C_j}{\partial T} \right) dT \end{aligned}$$

By multiplying the numerator and denominator by  $T$ , one can write the above equation in the form

$$\frac{dr_j}{r_j} = - \left( \frac{\partial R_j / R_j}{\partial T / T} + \frac{\partial C_j / C_j}{\partial T / T} \right) \frac{dT}{T} \quad (20)$$

Based on the assumption of homogeneity of elements of the same type for monolithic integrated circuits, it is reasonable to conclude that

$$\frac{dR_1}{R_1} = \frac{dR_2}{R_2} = \dots = \frac{dR_j}{R_j} = \dots = \frac{dR_n}{R_n} = \frac{dR}{R} \quad (21)$$

and

$$\frac{dC_1}{C_1} = \frac{dC_2}{C_2} = \dots = \frac{dC_j}{C_j} = \dots = \frac{dC_n}{C_n} = \frac{dC}{C} \quad (22)$$

Hence, Eq. 20 may be written

$$\frac{dr_j}{r_j} = - \left( \frac{\partial R/R}{\partial T/T} + \frac{\partial C/C}{\partial T/T} \right) \frac{dT}{T} \quad (23)$$

From Eq. 23, it follows that

$$\frac{dr_1}{r_1} = \frac{dr_2}{r_2} = \dots = \frac{dr_j}{r_j} = \dots = \frac{dr_n}{r_n} = \frac{dr}{r} \quad (24)$$

Thus Eq. 23 may be written

$$\frac{dr}{r} = - \left( S_T^R + S_T^C \right) \frac{dT}{T} \quad (25)$$

where from Eqs. 9 and 23,  $S_T^R$  and  $S_T^C$  are given by

$$S_T^R = \frac{\partial R/R}{\partial T/T} \quad (26)$$

$$S_T^C = \frac{\partial C/C}{\partial T/T} \quad (27)$$

If in Eq. 15, all of the open-loop poles,  $p_e$ , and zeros,  $z_k$ ,

are determined only by passive RC products, one can conclude the following, based on Eq. 25

$$\frac{dr}{r} = \frac{dp_e}{p_e} = \frac{dz_k}{z_k} \quad (28)$$

Thus, from Eq. 15, one obtains

$$\begin{aligned} dq_1 &= s_{T_0}^{q_1} \frac{dT_0}{T_0} + q_1 s_{T_0}^{q_1} \left( \sum_e \frac{1}{q_1 - p_e} - \sum_k \frac{1}{q_1 - z_k} \right) \frac{dr}{r} \\ &= s_{T_0}^{q_1} \frac{dT_0}{T_0} + q_1 \frac{dr}{r} \\ &= s_{T_0}^{q_1} \frac{dT_0}{T_0} - q_1 \left( s_{T_0}^R + s_{T_0}^C \right) \frac{dT}{T} \end{aligned} \quad (29)$$

where Eq. 17 has been used in the above derivation. Eq. 29 relates incremental changes in the closed-loop pole  $q_1$  to fractional changes in the low frequency value of the loop transmission,  $T_0$ , and to changes in the passive elements determining the open-loop poles and zeros with respect to fractional changes in temperature. It is convenient to introduce a multielement sensitivity for the closed-loop pole  $q_1$  defined according to

$$dq_1 = s_{T_0}^{q_1} \frac{dT_0}{T_0} + s_e^{q_1} s_T^e \frac{dT}{T} \quad (30)$$

where



$$S_e^{q_1} = -q_1 \quad (31)$$

$$S_T^e = S_T^R + S_T^C \quad (32)$$

Note that  $dq_1$ ,  $S_{T_0}^{q_1}$ , and  $S_e^{q_1}$  all have an associated phase while the remaining terms are scalars. By way of summation then, the incremental change,  $dq_1$ , of a closed-loop pole  $q_1$ , due to the sensitivity of passive elements to temperature can be described by a vector from the closed-loop pole  $q_1$  through the origin of magnitude  $|q_1| S_T^e \frac{dT}{T}$  where it is true that all open-loop poles and zeros are determined only by passive elements. #

### C. LOW FREQUENCY TEMPERATURE DEPENDENCE IN MONOLITHIC INTEGRATED CIRCUIT COMPONENTS

Recall that the closed-loop poles (natural frequencies) are also functions of the loop transmission gain constant,  $T_0$ , and that  $T_0$  is in general a function of active as well as passive elements. Thus, classical sensitivity may be used to relate fractional changes in  $T_0$  to fractional changes in temperature. If the hybrid-pi, small-signal transistor model of Fig. 4(a) is considered, it is apparent that  $T_0$  may

# The consequences of the non-realizability of the requirement that all open-loop singularities be determined only by passive RC products are examined in detail in Section III.

be expressed as a function of the following parameters

$$T_0 = T_0(R, \beta_0, \epsilon_m, r_\mu, r_o, r'_c) \quad (33)$$

where each of the parameters is assumed to be temperature sensitive and where the ohmic base resistance,  $r_x$ , is included in the general term  $R$  representing any passive, base-diffused resistor. Taking the total differential of Eq. 33 and rearranging terms, one obtains

$$\begin{aligned} \frac{dT_0}{T_0} &= \left( \frac{\partial T_0/T_0}{\partial R/R} \frac{\partial R/R}{\partial T/T} + \frac{\partial T_0/T_0}{\partial \beta_0/\beta_0} \frac{\partial \beta_0/\beta_0}{\partial T/T} + \frac{\partial T_0/T_0}{\partial \epsilon_m/\epsilon_m} \frac{\partial \epsilon_m/\epsilon_m}{\partial T/T} \right. \\ &\quad \left. + \frac{\partial T_0/T_0}{\partial r_\mu/r_\mu} \frac{\partial r_\mu/r_\mu}{\partial T/T} + \frac{\partial T_0/T_0}{\partial r_o/r_o} \frac{\partial r_o/r_o}{\partial T/T} + \frac{\partial T_0/T_0}{\partial r'_c/r'_c} \frac{\partial r'_c/r'_c}{\partial T/T} \right) \frac{dT}{T} \\ &= \left( s_{R/T}^{T_0} \frac{R}{T} + s_{\beta_0/T}^{T_0} \frac{\beta_0}{T} + s_{\epsilon_m/T}^{T_0} \frac{\epsilon_m}{T} + s_{r_\mu/T}^{T_0} \frac{r_\mu}{T} + s_{r_o/T}^{T_0} \frac{r_o}{T} + s_{r'_c/T}^{T_0} \frac{r'_c}{T} \right) \frac{dT}{T} \end{aligned} \quad (34)$$

$$= s_{T/T}^{T_0} \frac{dT}{T} \quad (35)$$

Note that in the above expressions, a summation of the contributions to the sensitivity of  $T_0$  from all elements of the same type within the circuit is implied by each term. If it is momentarily assumed that the dc biasing is such that collector currents to first-order are insensitive to temperature variations, the individual sensitivity functions in the above expression may be considered to be of two

types.<sup>#</sup> Terms relating the fractional changes in  $R$ ,  $\beta_0$ ,  $g_m$ ,  $r_\mu$ ,  $r_o$ , and  $r_c'$  to the fractional change in temperature are independent of any circuit configuration, whereas terms relating the fractional change in  $T_0$  to the fractional changes in  $R$ ,  $\beta_0$ ,  $g_m$ ,  $r_\mu$ ,  $r_o$ , and  $r_c'$  are dependent only on the circuit configuration considered.

In considering sensitivity functions of the first type above, Chenette<sup>18</sup> has reported typical temperature coefficients for  $\beta_0$  and  $R$  at 300°K of 6600 ppm/°C and 2000 ppm/°C respectively. These values may be related to the corresponding sensitivity functions by the expression

$$S_T^x = T \gamma_T^x \quad (36)$$

Thus

$$S_T^{\beta_0} = 2.0$$

$$S_T^R = 0.6$$

The expression for the transconductance  $g_m$  is

---

<sup>#</sup> In terms of the four possible combinations of two two-port networks in a feedback configuration, it can be demonstrated that the shunt-series combination and, where the load and feedback function have similar temperature dependence, the shunt-shunt combination stabilize current gain in the feedback loop with respect to temperature. Circuits considered throughout the remainder of this report will be restricted to these configurations.

$$-\xi_m = \frac{qI_C}{kT} \quad (37)$$

Thus from Eq. 9, the sensitivity function is given by

$$S_T^{\xi_m} = S_T^{I_C} - 1.0 \quad (38)$$

Suppose that a bias scheme is chosen such that dc collector current is stabilized with respect to temperature. Eq. 38 then reduces to

$$S_T^{\xi_m} = -1.0$$

The output resistance,  $r_o$ , is given by

$$r_o = \frac{1}{\xi_m \eta} \quad (39)$$

where the basewidth modulation factor,  $\eta$ , is proportional to  $kT/q$ . The sensitivity function is then given by

$$S_T^{r_o} = -S_T^{I_C} \quad (40)$$

where it is assumed that contributions to the sensitivity of  $r_o$  due to variations in basewidth with respect to collector-base voltage are of second order.<sup>19</sup> Again where  $I_C$  is stabilized with respect to temperature, Eq. 40 reduces to

$$s_T^{r_o} = 0$$

Next,  $r_\mu$  can be obtained from the product of  $\beta_o$  and  $r_o$ <sup>#</sup>

$$r_\mu = \beta_o r_o \quad (41)$$

The sensitivity function for  $r$  is thus given by

$$s_T^{r_\mu} = s_T^{\beta_o} - s_T^{I_C} \quad (42)$$

Again, where  $I_C$  is stabilized with respect to temperature,

$$s_T^{r_\mu} = s_T^{\beta_o} \quad (43)$$

$$= 2.0$$

Finally, recall that  $r_o'$  models bulk resistance effects in the collector region, which is usually lightly doped.

---

<sup>#</sup> The expression for  $r_\mu$  is correct if it is assumed that the bulk recombination defect is large with respect to the emitter efficiency defect.<sup>19</sup> This assumption is not justified for planar, diffused structures currently being produced. A more correct expression would seem to be  $r_\mu = \beta_o' r_o$  where  $\beta_o' \gg \beta_o$ . An attempt to verify this by considering manufacturers h-parameter and y-parameter data was unsuccessful in that computed ratios of  $r_\mu/r_o$  varied from values much less than  $\beta_o$  to values much greater than  $\beta_o$ . Because of this lack of agreement and because  $r_\mu$  is large in any case and its effects relatively negligible, the functional relationship of Eq. 41 is assumed.

Its value and temperature coefficient can vary depending on whether or not a buried layer is used. It is assumed that the temperature coefficient is approximately<sup>#</sup>

$$\gamma_{T}^{r'_c} = 3000 \text{ ppm}/^{\circ}\text{C}$$

at 300°K. The sensitivity function is thus given by

$$S_{T}^{r'_c} = 0.9$$

These results are summarized in Table 2.

Though expressions for  $T_0$  do not involve charge storage elements, for completeness, they are considered briefly.

The elements  $c_{\mu}$  and  $c_s$  are assumed constant with temperature, while  $c_{\pi}$  is assumed to have the same temperature dependence as  $\epsilon_m$ , where  $f_t$  is assumed constant with temperature.

The second group of sensitivity functions (those relating the fractional change in  $T_0$  to the fractional changes in  $R$ ,  $\beta_0$ ,  $\epsilon_m$ ,  $r_{\mu}$ ,  $r_0$ , and  $r'_c$ ) are dependent on actual circuit configurations. Note that in any single-loop feedback formulation,  $T_0$  is a dimensionless quantity even though  $a(0)$  and  $f(0)$  may not be dimensionless. It is

---

<sup>#</sup> The consensus conveyed to the author in recent private conversations with several people more closely involved in the processing area is that the temperature coefficient of  $r'_c$  should actually be somewhat less than that for a base-diffused resistor. The functional dependence assumed here was retained, however, as these conversations occurred after the compilation of this report and as it was felt that this correction would not significantly alter the results and conclusions presented.

Table 2

Typical First-Order Parameter Sensitivities

x	$S_T^x$	$S_T^x \Big _{I_C \neq f(T)}$
R	0.6	0.6
$B_O$	2.0	2.0
$g_m$	$S_T^{I_C} - 1.0$	1.0
$r_o$	$-S_T^{I_C}$	0
$r_\mu$	$2.0 - S_T^{I_C}$	2.0
$r'_c$	0.9	0.9

convenient then to consider three examples in which the sensitivity of voltage and current gain are examined. It is assumed that  $I_C$  is stabilized with respect to temperature.

In the common-emitter configuration of Fig. 5(a), charge storage elements have been neglected since only the low-frequency value of voltage gain is of interest for the moment. If  $r_x$  is assumed to be included in  $R_s$  and the effects of  $r_\mu$ ,  $r_o$ , and  $r_c^i$  are assumed to be negligible, the circuit of Fig. 5(a) reduces to that of Fig. 5(b). The low frequency value of voltage gain is then

$$\begin{aligned}
 a_v(0) &= \frac{V_L}{V_S} = -a_{v0} = \frac{-\beta_0 R_L}{R_s + \beta_0 / g_m + (\beta_0 + 1) R_e} \\
 &\approx \frac{-R_L}{R_s / \beta_0 + 1 / g_m + R_e} \quad (44)
 \end{aligned}$$

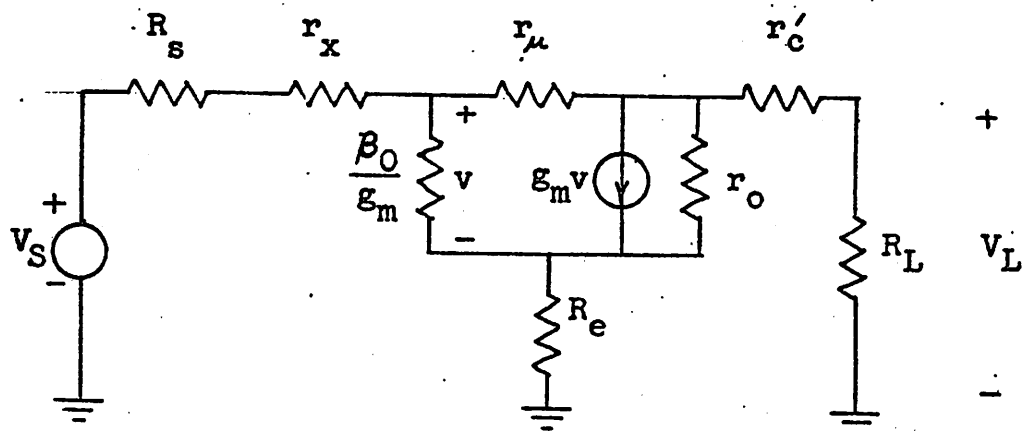
Taking the total differential of Eq. 44 with respect to temperature and rearranging terms, one obtains

$$\frac{da_v(0)}{a_v(0)} = \frac{(R_s / \beta_0) S_T^{\beta_0} + (1 / g_m) (S_T^{g_m} + S_T^R)}{R_s / \beta_0 + 1 / g_m + R_e} \frac{dT}{T}$$

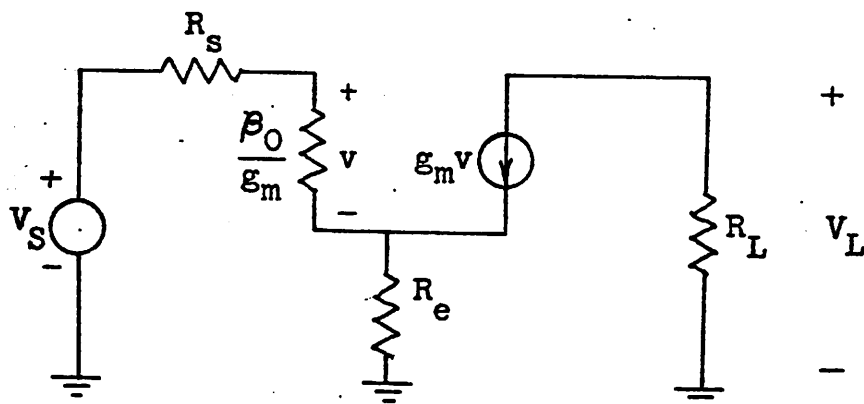
The sensitivity function is thus

$$S_T^{a_v(0)} = \frac{(R_s / \beta_0) S_T^{\beta_0} + (1 / g_m) (S_T^{g_m} + S_T^R)}{R_s / \beta_0 + 1 / g_m + R_e} \quad (45)$$

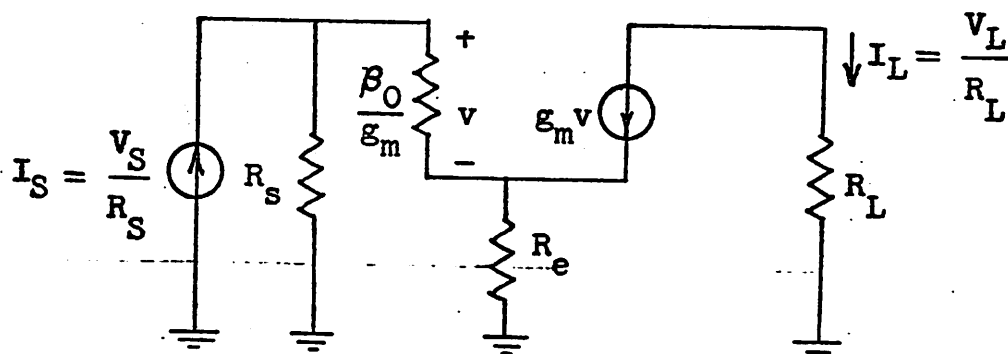




(a)



(b)



(c)

Fig. 5. (a) Low-frequency, small-signal representation of a c-e stage. (b) First-order approximation to circuit (a). (c) Circuit (b) with Norton equivalent source.

From Eq. 45, individual sensitivity functions may be extracted and the equation put in the form of Eq. 34; however, it is more convenient to leave the expression in its present form.

As typical values, assume  $R_s = 5 \text{ k}\Omega$ ,  $R_e = 10 \text{ }\Omega$ ,  $R_L = 5 \text{ k}\Omega$ ,  $\beta_o = 100$ , and  $r_e = g_m^{-1} = 12.5 \text{ }\Omega$ ; then

$$a_v(0) = \frac{-5000}{(50 + 12.5 + 10)} = -69.0$$

and

$$\begin{aligned} s_T a_v(0) &= \frac{50s_T \beta_o + 12.5(s_T g_m + s_T R)}{72.5} \\ &= 1.31 \end{aligned}$$

At  $T = 300^\circ\text{K}$ , the temperature coefficient is

$$\gamma_T^{a_v(0)} = 4360 \text{ ppm}/^\circ\text{C}$$

If in the circuit of Fig. 5(b) the source is replaced by its Norton equivalent, the low frequency value of current gain is then, from Eq. 44,

$$a_I(0) = \frac{-I_L}{I_S} = \frac{V_L R_s}{V_S R_L} = a_{IO}$$

$$\approx \frac{-R_s}{R_s/\beta_o + 1/g_m + R_e} \quad (46)$$

The sensitivity function is obtained in a manner similar to that for voltage gain and is found to be

$$\begin{aligned} \frac{a_I(0)}{S_T} &= \frac{a_v(0)}{S_T} \\ &= \frac{(R_S/\beta_o)S_T^{\beta_o} + (1/g_m)(S_T^{g_m} + S_T^R)}{R_S/\beta_o + 1/g_m + R_e} \end{aligned} \quad (47)$$

Thus for the typical element values assumed

$$a_I(0) = -69.0$$

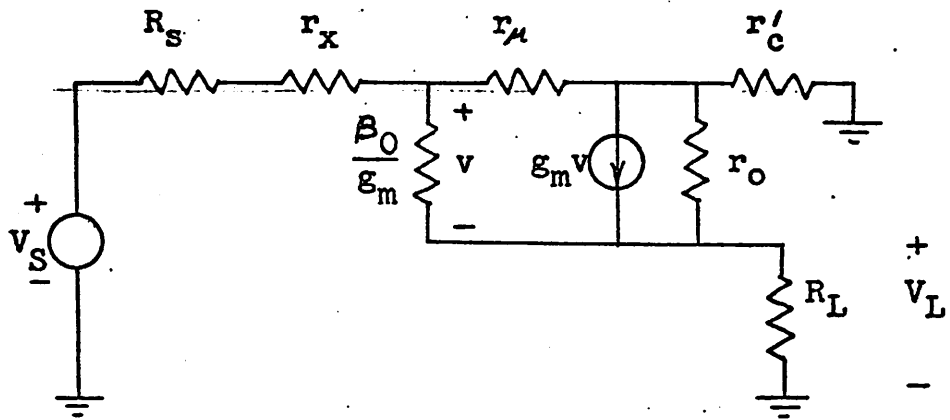
$$\frac{a_I(0)}{S_T} = 1.31$$

Next consider the emitter follower of Fig. 6(a).

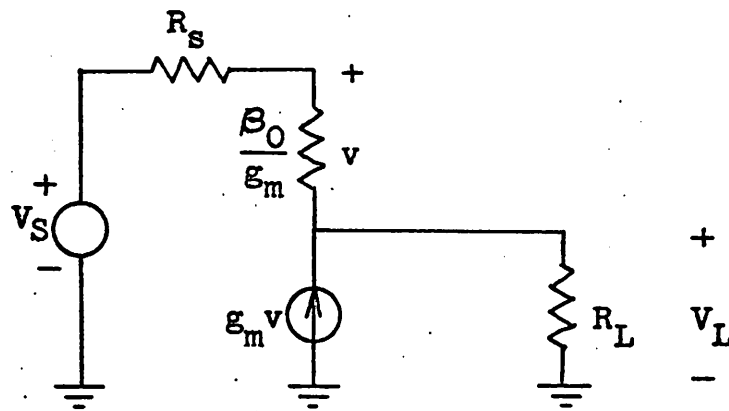
Again if  $r_x$  is absorbed into  $R_S$  and if  $r_{\mu}$ ,  $r_o$ , and  $r'_c$  neglected, the circuit of Fig. 6(a) reduces to that of Fig. 6(b). The low frequency value of the voltage gain is given by

$$\begin{aligned} a_v(0) &= \frac{V_L}{V_S} = a_{vo} = \frac{(\beta_o + 1)R_L}{R_S + \beta_o/g_m + (\beta_o + 1)R_L} \\ &\approx \frac{R_L}{R_S/\beta_o + 1/g_m + R_L} \end{aligned} \quad (48)$$

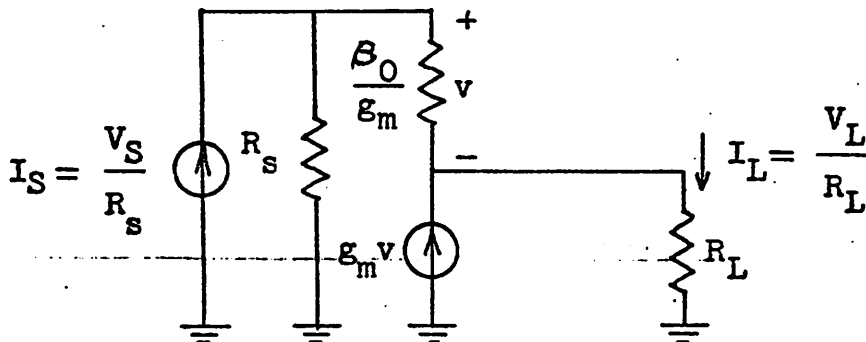
Taking the total differential of Eq. 48 with respect to temperature and rearranging terms, one obtains



(a)



(b)



(c)

Fig. 6. (a) Low-frequency, small-signal representation of an emitter follower stage. (b) First-order approximation to circuit (a). (c) Circuit (b) with Norton equivalent source.

$$\frac{da_v(0)}{a_v(0)} = \frac{(R_s/\beta_o)S_T^{\beta_o} + (1/g_m)(S_T^{g_m} + S_T^R) dT}{R_s/\beta_o + 1/g_m + R_L} \frac{dT}{T}$$

Thus the sensitivity function is

$$S_T^{a_v(0)} = \frac{(R_s/\beta_o)S_T^{\beta_o} + (1/g_m)(S_T^{g_m} + S_T^R)}{R_s/\beta_o + 1/g_m + R_L} \quad (49)$$

Assume  $R_s = 5 \text{ k}\Omega$ ,  $R_L = 3 \text{ k}\Omega$ ,  $\beta_o = 100$ , and  $r_e = g_m^{-1} = 50 \Omega$ ; then

$$a_v(0) = \frac{3000}{(50 + 50 + 3000)} = 0.97$$

and

$$\begin{aligned} S_T^{a_v(0)} &= \frac{50S_T^{\beta_o} + 50(S_T^{g_m} + S_T^R)}{3100} \\ &= 0.026 \end{aligned}$$

At  $300^\circ\text{K}$ , the temperature coefficient is

$$\gamma_T^{a_v(0)} = 86 \text{ ppm}/^\circ\text{C}$$

The circuit of Fig. 6(c) is obtained by replacing the source in the circuit of Fig. 6(b) by its Norton equivalent. The low frequency value of current gain is given by

$$a_I(0) = \frac{I_L}{I_S} = a_v(0) \frac{R_s}{R_L} = a_{IO}$$

$$a_I(0) \approx \frac{R_s}{R_s/\beta_o + 1/g_m + R_L} \quad (50)$$

where Eq. 48 has been used. The sensitivity function is given by

$$\begin{aligned} S_T^{a_I(0)} &= S_T^{a_v(0)} \\ &= \frac{R_s/\beta_o S_T^{\beta_o} + (1/g_m)(S_T^{g_m} + S_T^R)}{R_s/\beta_o + 1/g_m + R_L} \end{aligned} \quad (51)$$

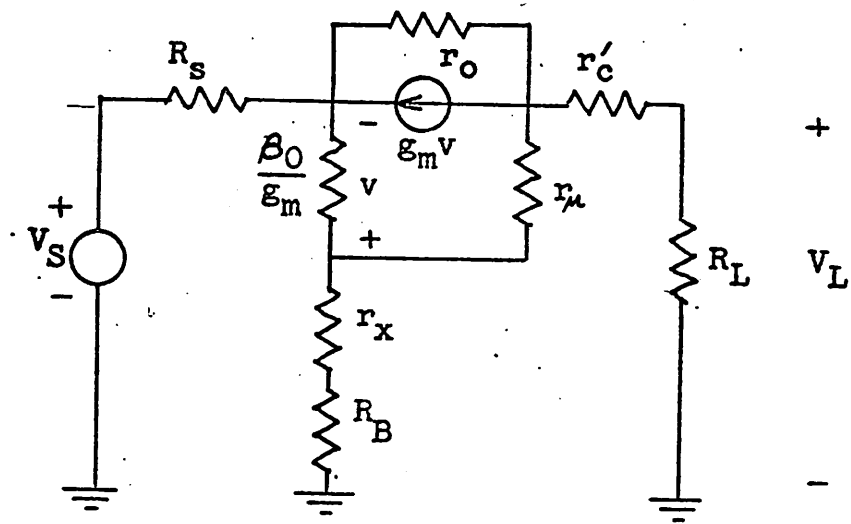
For the typical element values assumed

$$a_I(0) = 1.61$$

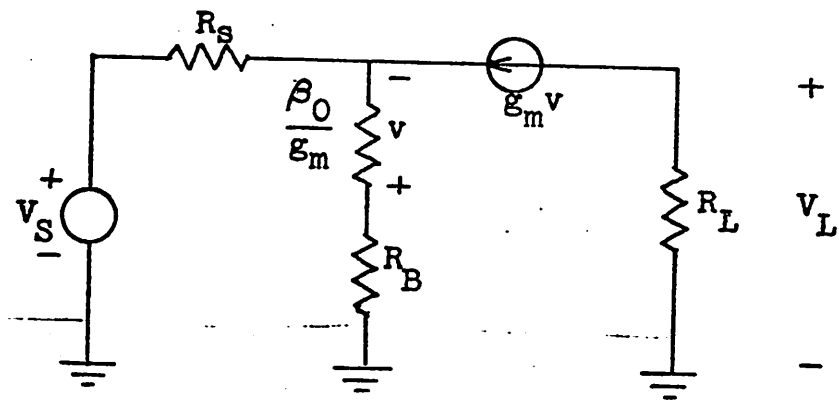
$$\frac{a_I(0)}{S_T} = 0.026$$

Finally, as a third example, consider the common-base configuration of Fig. 7(a). Absorbing  $r_x$  into  $R_B$  and neglecting  $r_\mu$ ,  $r_o$  and  $r'_c$ , one obtains the circuit of Fig. 6(b). The low-frequency value of the voltage gain is given by

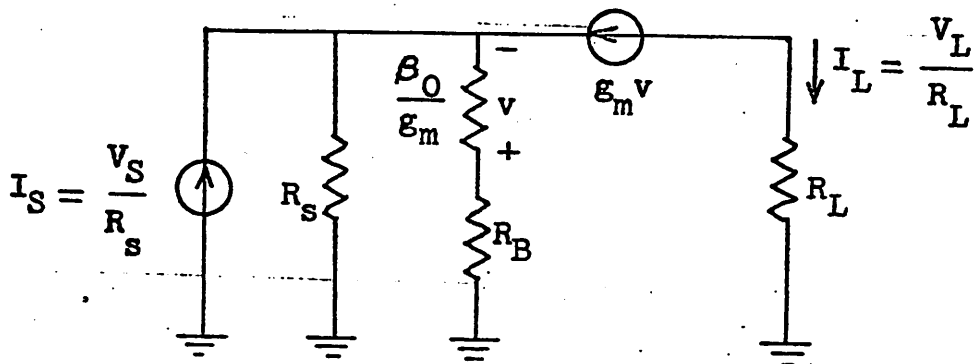
$$\begin{aligned} a_v(0) &= \frac{V_L}{V_S} = a_{vo} = \frac{(\beta_o + 1)R_L}{R_B + \beta_o/g_m + (\beta_o + 1)R_s} \\ &\approx \frac{R_L}{R_B/\beta_o + 1/g_m + R_s} \end{aligned} \quad (52)$$



(a)



(b)



(c)

Fig. 7. (a) Low-frequency, small signal representation of a c-b stage. (b) First-order approximation to circuit (a). (c) Circuit (b) with Norton equivalent source.

Upon taking the total differential of Eq. 52 with respect to temperature and rearranging terms in the usual manner, one obtains the sensitivity function

$$S_T^{a_v(0)} = \frac{R_B/\beta_o S_T^{\beta_o} + (1/g_m)(S_T^{g_m} + S_T^R)}{R_B/\beta_o + 1/g_m + R_s} \quad (53)$$

Assume  $R_s = 400 \Omega$ ,  $R_B = 10 \text{ k}\Omega$ ,  $R_L = 2 \text{ k}\Omega$ ,  $\beta_o = 100$ , and  $r_e = g_m^{-1} = 25 \Omega$ ; then

$$a_v(0) = \frac{2000}{(100 + 25 + 400)} = 3.81$$

$$\begin{aligned} S_T^{a_v(0)} &= \frac{100 S_T^{\beta_o} + 25(S_T^{g_m} + S_T^R)}{525} \\ &= 0.362 \end{aligned}$$

At  $300^\circ\text{K}$ , the temperature coefficient is

$$\gamma_T^{a_v(0)} = 1200 \text{ ppm}/^\circ\text{C}$$

The circuit of Fig. 7(c) is again obtained by replacing the source in the circuit of Fig. 7(b) by its Norton equivalent. The low-frequency value of current gain is given by

$$a_I(0) = \frac{I_L}{I_S} = a_v(0) \frac{R_s}{R_L} = a_{IO} \quad (54)$$

$$\approx \frac{R_s}{R_B/\beta_o + 1/g_m + R_s} \quad (55)$$



where Eq. 52 has been used. The sensitivity function is given by

$$\begin{aligned} \frac{a_I(0)}{S_T} &= \frac{a_v(0)}{S_T} \\ &= \frac{R_B/\beta_o S_T^{\beta_o} + (1/g_m)(S_T^{g_m} + S_T^R)}{R_B/\beta_o + 1/g_m + R_s} \end{aligned} \quad (56)$$

For the typical element values assumed

$$a_I(0) = 0.76$$

$$\frac{a_I(0)}{S_T} = 0.362$$

#### D. PARTIALLY COMPENSATED SELECTIVE AMPLIFIER

At this point it will be helpful to begin to tie some of the results and conclusions from above together. Recall that response invariance is of primary concern. Response invariance in terms of constant center frequency,  $\omega_o$ , and constant bandwidth, BW, is obtained if the net displacement of the dominant complex pair of poles (natural frequencies) is zero, as will be shown below. Subject to the assumption that all open-loop poles and zeros are determined only by passive RC products, the displacement of the closed-loop pole  $q_1$  can be written from Eqs. 30 and 35 as follows

$$dq_1 = S_{T_0}^{q_1} S_{T_0}^{T_0} \frac{dT}{T} + S_e^{q_1} S_e^e \frac{dT}{T} \quad (57)$$

$$= \left( S_{T_0}^{q_1} S_{T_0}^{T_0} + S_e^{q_1} S_e^e \right) \frac{dT}{T} \quad (58)$$

The first term relates incremental changes of  $q_1$  along the original locus to changes in the loop transmission gain constant,  $T_0$ , with respect to fractional changes in temperature. The second term relates incremental changes in the shape of the original locus of the closed-loop pole  $q_1$  to changes in the passive elements determining the open-loop poles and zeros with respect to fractional changes in temperature.

Let  $q_1$  denote one of the dominant complex pair of closed-loop poles.<sup>#</sup> If it is assumed that a narrow-band situation exists, the center frequency can be approximated by

$$\omega_0 \approx \text{Im}(q_1) \quad (59)$$

and from Eqs. 9 and 58, one obtains

$$S_T^{\omega_0} = \frac{\partial \text{Im}(q_1) / \text{Im}(q_1)}{\partial T/T} = S_T^{\text{Im}(q_1)} \quad (60)$$

<sup>#</sup> It will be understood that any conclusions drawn regarding the behavior of  $q_1$  also apply to its conjugate denoted  $q_2$ .

$$S_T^{\omega_0} = \frac{S_{T_0}^{T_0} \operatorname{Im}(S_{T_0}^{q_1})}{\operatorname{Im}(q_1)} + \frac{S_T^e \operatorname{Im}(S_e^{q_1})}{\operatorname{Im}(q_1)} \quad (61)$$

Under similar conditions, from Eq. 7, one can approximate the bandwidth by

$$BW \approx -2\operatorname{Re}(q_1) \quad (62)$$

and from Eqs. 9 and 58, one obtains

$$S_T^{BW} = \frac{\partial 2\operatorname{Re}(q_1)/2\operatorname{Re}(q_1)}{\partial T/T} = S_T^{\operatorname{Re}(q_1)} \quad (63)$$

$$= \frac{S_{T_0}^{T_0} \operatorname{Re}(S_{T_0}^{q_1})}{\operatorname{Re}(q_1)} + \frac{S_T^e \operatorname{Re}(S_e^{q_1})}{\operatorname{Re}(q_1)} \quad (64)$$

It is apparent from Eqs. 60 and 63 that if  $dq_1 = 0$ , response invariance is achieved.

The condition  $dq_1 = 0$  is satisfied if and only if

$$S_{T_0}^{q_1} S_{T_0}^{T_0} = -S_e^{q_1} S_T^e \quad (65)$$

This expression may be written in terms of magnitude and phase as

$$\left| S_{T_0}^{q_1} \right| \left| S_{T_0}^{T_0} \right| = \left| S_e^{q_1} \right| \left| S_T^e \right| \quad (66a)$$

$$\operatorname{Arg} \left( S_{T_0}^{q_1} S_{T_0}^{T_0} \right) = -\operatorname{Arg} \left( S_e^{q_1} S_T^e \right) \quad (66b)$$

Three of the four terms in Eq. 65 have been considered in some detail. The fourth,  $S_{T_0}^{q_1}$ , has been mentioned only briefly (Eq. 16). It is considered in detail in Appendix A, and specific examples are considered shortly. One important conclusion can be reached immediately without any further detailed analysis. Recall that the basic concept behind root-locus techniques is to illustrate the trajectory of a closed-loop pole as  $T_0$  (or  $f(0)$ ) is changed. If the incremental change,  $dq_1$ , of any closed-loop pole  $q_1$  is considered in terms of its magnitude and phase, the phase must be such that the pole moves along a tangent to the locus at the point  $q_1$ . Further recall that the phase of  $S_e^{q_1}$  is determined by the angle of a vector from  $q_1$  through the origin of the complex frequency plane. From examples considered in the previous section, it is apparent that generally  $S_T^{T_0} > 0$ . Further, it is generally true that  $S_T^e > 0$ . The phase condition, Eq. 66(b), then reduces to

$$\text{Arg } S_{T_0}^{q_1} = - \text{Arg } S_e^{q_1} \quad (67)$$

This condition can only be satisfied when the tangent to the root locus at the point  $q_1$  passes directly through the origin.

The consequences of the above conclusion with regard to the two-pole example of Section I.A are immediately apparent. The phase condition can never be satisfied for a complex

pair of closed-loop poles in the open left-half plane. Partial compensation in terms of constant center frequency can be achieved, however, as the following example will show.

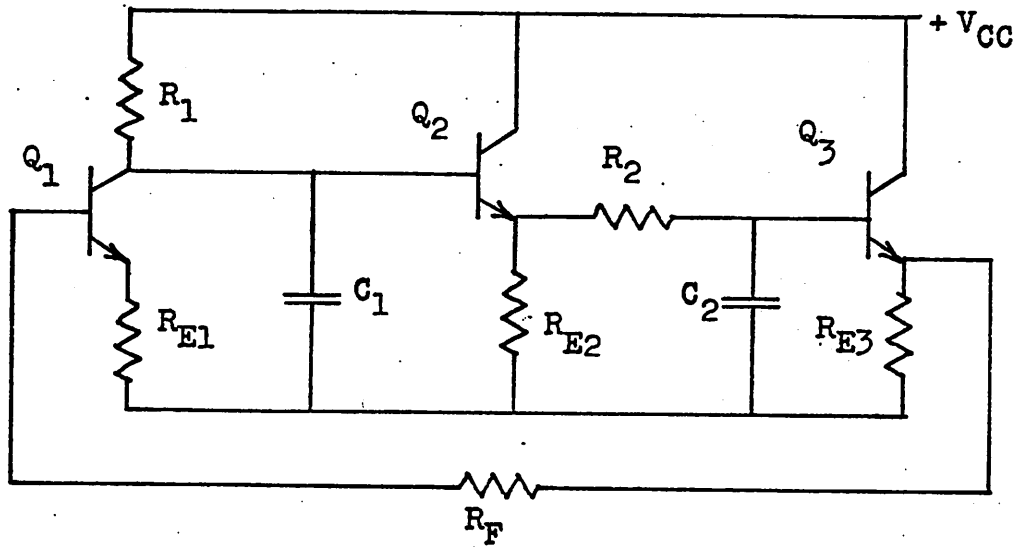
Consider the negative feedback amplifier of Fig. 8. It consists of a single inverting common emitter stage and two emitter followers. This configuration was designed to provide good isolation between active devices and those passive RC elements used to determine the dominant open-loop singularities. In a small-signal representation, the high output impedance of the common emitter stage and the high input impedance of the first emitter follower effectively isolate  $R_1$  and  $C_1$  from the rest of the circuit. One open-loop pole is thus given by

$$p_1 = -1/R_1 C_1 \quad (68)$$

Similarly, the low output impedance of the first emitter follower and the high input impedance of the second emitter follower effectively isolate  $R_2$  and  $C_2$  from the rest of the circuit. The second open-loop pole is thus given by

$$p_2 = -1/R_2 C_2 \quad (69)$$

To first-order, the requirement that all dominant open-loop poles and zeros be determined by passive RC products has been satisfied. The characteristic polynomial of the closed-loop transfer function can be written directly by inspection



$R_1 = 5 \text{ k}\Omega$	$R_{E1} = 10 \Omega$	$V_{CC} = 12.5 \text{ V}$
$C_1 = 100 \text{ pF}$	$R_{E2} = 3 \text{ k}\Omega$	$I_{C1} = 2.0 \text{ mA}$
$R_2 = 5 \text{ k}\Omega$	$R_{E3} = 3 \text{ k}\Omega$	$I_{C2} = 0.5 \text{ mA}$
$C_2 = 100 \text{ pF}$	$R_F = 5 \text{ k}\Omega$	$I_{C3} = 0.25 \text{ mA}$

Fig. 8. A partially compensated two pole negative feedback frequency selective amplifier.

as#

$$s^2 + \left( \frac{1}{R_1 C_1} + \frac{1}{R_2 C_2} \right) s + \frac{T_0 + 1}{R_1 R_2 C_1 C_2} = 0 \quad (70)$$

where

$$T_0 = -a(0)f(0) \quad (71)$$

Assume

$$p = p_1 = p_2 = -1/RC \quad (72)$$

Then Eq. 70 may be written

$$s^2 - 2ps + p^2(1 + T_0) = 0 \quad (73)$$

From Eq. 73, the poles of the closed-loop transfer function and the dominant natural frequencies of the circuit of Fig.

8 are given by

$$q_{1,2} = p \pm jp\sqrt{T_0} \quad (74)$$

---

# A question might arise as to whether a possible Miller effect augmentation of the effects of  $c_{\mu}$  could lead to severe distortion of the expected root loci. Curiously enough, for both first-order ( $c_{\pi}$  and  $c_{\mu}$  now included) and second-order representations, the following was observed upon using computer analysis. When  $C_1$  and  $C_2$  were present, there appeared to be no Miller effect augmentation. When  $C_1$  and  $C_2$  were removed, an open-loop pole due to  $c_{\mu}$  appeared in the vicinity of  $-2.5 \times 10^6$  rad/sec. The explanation seems to lie in the fact that Miller effect arguments are based on characteristic time constant descriptions which cannot adequately describe any but the most dominant natural frequency.

The center frequency,  $\omega_0$ , and the bandwidth, BW, are given by

$$\omega_0 = -p\sqrt{T_0} \quad (75)$$

$$BW = -2p \quad (76)$$

To this point,  $a(0)$  and  $f(0)$  have not been identified. Assume that the voltage at the emitter of  $Q_3$  is taken as the output and that the input signal is applied at the base of  $Q_1$ . The natural feedback description is in terms of a shunt-shunt combination, and  $a(0)$  is recognized as a transimpedance while  $f(0)$  is the transadmittance  $-1/R_F$ . Recall that for shunt-shunt feedback, transimpedance is made insensitive. If in the circuit of Fig. 8 both  $R_F$  and  $R_{E3}$ , the effective load resistance, are considered to be diffused resistors, it can be assumed that they will exhibit similar temperature dependence, and thus current gain can also be considered stabilized with respect to temperature as desired.  $T_0$  is a current gain and is easily evaluated by inspection by considering the voltage gain from the collector of  $Q_1$  around the loop and then making the conversion to current gain. If the first-order, low-frequency, small-signal hybrid-pi model of Fig. 4(b) is substituted and it is assumed that the load seen by each emitter follower is  $3 \text{ k}\Omega$ , application of the gain expressions developed in Section I.C yields



$$T_0 = -a_v(0) \frac{R_1}{R_L'} \approx 64 \quad (77)$$

where  $R_L'$  is an equivalent low frequency driving point resistance seen from the collector of  $Q_1$ . Thus center frequency, bandwidth, and selectivity are given by

$$\omega_0 \approx 16 \times 10^6 \text{ rad/sec}$$

$$\text{BW} \approx 4 \times 10^6 \text{ rad/sec}$$

$$Q \approx 4$$

Consider now the expression for the incremental displacement of the closed-loop pole  $q_1$ . From Eq. 58

$$dq_1 = \left( s_{T_0}^{q_1} s_T^{T_0} - q_1 s_T^R \right) \frac{dT}{T} \quad (78)$$

where it is assumed  $s_T^C = 0$ . From Eq. 74

$$s_{T_0}^{q_1} = \frac{1}{2} j p \sqrt{T_0} \quad (79)$$

Thus Eq. 78 may be written

$$dq_1 = \left( \frac{1}{2} j p \sqrt{T_0} s_T^{T_0} - q_1 s_T^R \right) \frac{dT}{T} \quad (80)$$

From Eqs. 61 and 64 and from Eq. 74

$$S_{T}^{\omega_0} = \frac{1}{2} S_{T}^{\omega_0} - S_{T}^R \quad (81)$$

$$S_{T}^{BW} = - S_{T}^R \quad (82)$$

Again, from examples considered previously and from Eqs. 81 and 82, one obtains

$$S_{T}^{\omega_0} \approx 0.655 - 0.6 = 0.055$$

and

$$S_{T}^{BW} \approx -0.6$$

At 300°K, these values correspond to temperature coefficients of

$$\gamma_{T}^{\omega_0} \approx 175 \text{ ppm/}^\circ\text{C}$$

$$\gamma_{T}^{BW} \approx -2000 \text{ ppm/}^\circ\text{C}$$

These predicted results may be compared to those obtained by computer analysis of the circuit of Fig. 8 and presented in Table 3. Element values were varied according to the results of Table 2 to reflect variations over a 5°C temperature change. The results of the second column are based on the transistor representation of Fig. 4(b) and give good agreement. The results of the third column are

Table 3

Temperature Dependence of a Partially Compensated Two Pole, Negative Feedback, Frequency Selective Amplifier (Frequency in rad/sec x 10<sup>6</sup>. Sensitivity in ppm/°C.)

	Design	First-Order	Second-Order
$p_1$	-2.00	-1.84	-1.32
$p_2$	-2.00	-2.23	-2.04
$T_0$	64.0	62.3	52.3
$\gamma_T^{T_0}$	+4350	+4390	+4820
$q_{1,2}$	$-2.00 \pm j16.00$	$-2.04 \pm j16.01$	$-0.716 \pm j11.84$
$\omega_0$	16.00	16.01	11.84
$\gamma_T^{\omega_0}$	+175	+50	-865
BW	4.00	4.08	1.43
$\gamma_T^{BW}$	-2000	-2140	-8000
Q	4.00	3.92	8.26
$\gamma_T^Q$	+1825	+2090	+7135

based on the transistor representation of Fig. 4(a). Here there is a significant deviation from predicted results in terms of both closed-loop pole location and sensitivity. This is primarily due to excess phase resulting from the additional open-loop poles and zeros present when charge storage is considered. The nearest open-loop pole is on the negative real axis at  $-74.9 \times 10^6$  rad/sec. This pole results largely from  $c_{\pi}$  ( $\approx 20.2$  pF) associated with  $Q_1$ . This is demonstrated by the fact that when  $c_{\pi}$  is removed from the circuit, the nearest open-loop pole is found to be at  $-331.9 \times 10^6$  rad/sec. In Fig. 9 two root loci of the closed-loop poles  $q_{1,2}$  are shown. The first (dashed curve) corresponds to the simple two pole approximation associated with the first-order analysis of the second column of Table 3. The second (solid curve) corresponds to the addition of the nearest non-dominant pole indicated above to the two open-loop poles given in the third column of Table 3. It can be seen that this second locus reflects the closed-loop response found in Table 3. The additional open-loop pole then adequately models the effects of excess phase.

It is apparent from the previous discussions and this example that sufficient degrees of design freedom (sufficient control of the shape of the root locus) to allow the simultaneous realization of a desired response and its invariance with respect to temperature are not available with a system whose open-loop transfer function can be

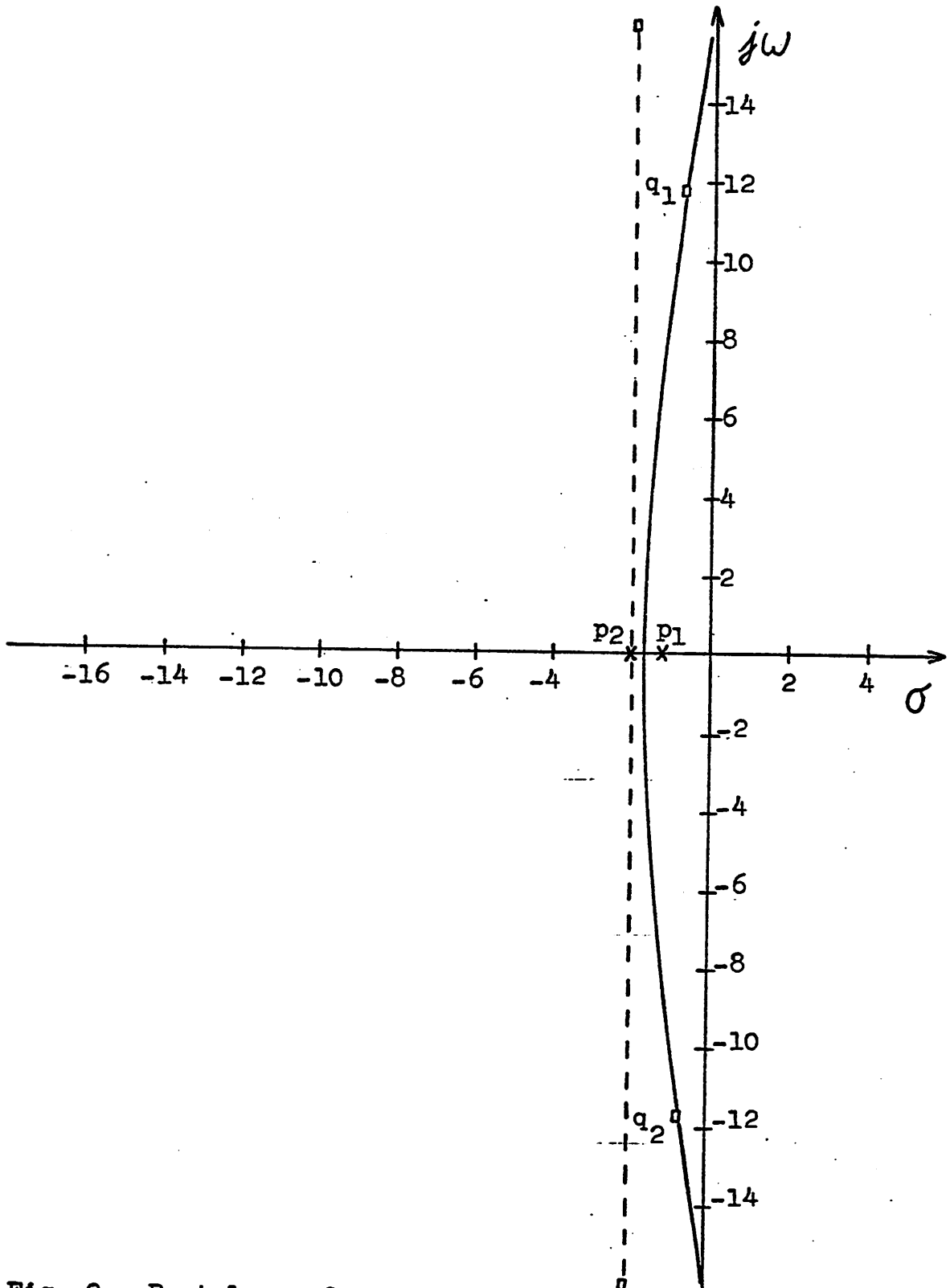


Fig. 9. Root locus for a first-order analysis of a two pole negative feedback selective amplifier (dashed curve) and the effects of excess phase (solid curve).

approximated by two dominant poles. In the next section, systems with additional degrees of freedom are examined. These additional degrees of freedom appear as additional open-loop poles and zeros.

## II. COMPENSATION WITH ADDITIONAL DEGREES OF FREEDOM

It has been pointed out that a frequency selective feedback amplifier whose open-loop transfer function can be approximated by two dominant poles does not have sufficient degrees of freedom to satisfy the phase condition, Eq. 67, for zero sensitivity of the closed-loop poles  $q_{1,2}$ . This limitation can be examined in a more quantitative manner. Recall that the poles of  $A(s)$  are given by the zeros of  $1 + T(s)$ , where  $T(s)$  is given by either Eq. 11 or Eq. 12. From Eq. 12, it follows that the necessary phase condition for  $q_1$  to be a closed-loop pole of  $A(s)$  is given by

$$\sum_k \text{Arg} (q_1 - z_k) - \sum_e \text{Arg} (q_1 - p_e) = \pi \quad (83)$$

If the following notation is adopted,

$$\hat{r}_j = \text{Arg} (q_1 - r_j) \quad (84)$$

Eq. 83 may be written in the form

$$\sum_k \hat{z}_k - \sum_e \hat{p}_e = \pi \quad (85)$$

The phase condition for zero sensitivity of the closed-loop pole  $q_1$  can be obtained from Eq. 67

$$\text{Arg } S_{T_0}^{q_1} = - \text{Arg } S_e^{q_1} \quad (86)$$

$$= - \text{Arg } (-q_1) = \pi/2 + \delta \quad (87)$$

where  $\delta$  is defined in Fig. 10 and is given by

$$\delta = - \text{Tan}^{-1} \frac{\text{Re } (q_1)}{\text{Im } (q_1)} \quad (88)$$

From Eq. 16,  $S_{T_0}^{q_1}$  can be written

$$S_{T_0}^{q_1} = \frac{\prod_e (q_1 - p_e)}{\prod_{j=2}^m (q_1 - q_j)} \quad (89)$$

From Eqs. 87 and 89 and from Eq. 85, repeated here, the two independent phase conditions which must be satisfied at  $q_1$  are

$$-\sum \hat{z}_k - \sum \hat{p}_e = \pi \quad (85)$$

$$\sum \hat{p}_e - \sum \hat{q}_j = \pi/2 + \delta \quad (90)$$

Consider again the two pole example previously discussed. From Eq. 85, one obtains

$$-(\hat{p}_1 + \hat{p}_2) = \pi$$



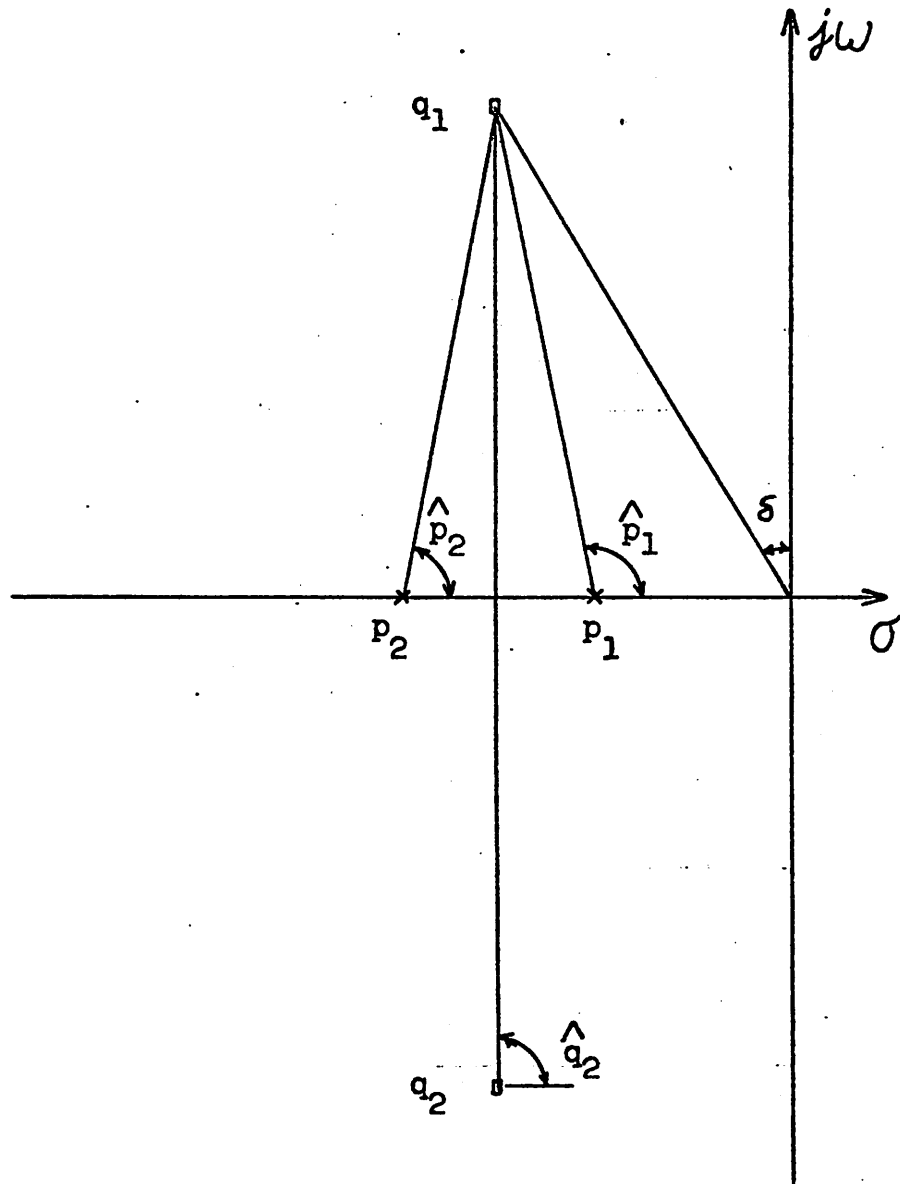


Fig. 10. Phase angles associated with the root locus.

and from Eq. 90, one obtains

$$\hat{p}_1 + \hat{p}_2 - \pi/2 = \pi/2 + \delta$$

A unique solution for  $\delta$  exists

$$\delta = -2\pi = 0$$

This result indicates that the root locus must include the entire imaginary axis, which is the conclusion reached before from physical reasoning.

Consider now the open-loop pole-zero configuration and root locus plot of Fig. 11 where a single zero has been added to the system previously considered. From Eqs. 85 and 90, one obtains

$$\hat{z}_1 - \hat{p}_1 - \hat{p}_2 = \pi \quad (91)$$

and

$$\hat{p}_1 + \hat{p}_2 - \pi/2 = \pi/2 + \delta \quad (92)$$

It is apparent that the additional degree of freedom resulting from the added zero allows the simultaneous solution of these two equations for an arbitrary choice of  $\delta$ . By way of example, assume  $f_o = 79.5$  kHz. and  $Q = 50$ ; then the required values of  $q_{1,2}$  and  $\delta$  are given by

$$q_{1,2} = (-0.005 \pm j 0.5) \times 10^6 \text{ rad/sec}$$

$$\delta = 0.573^\circ$$

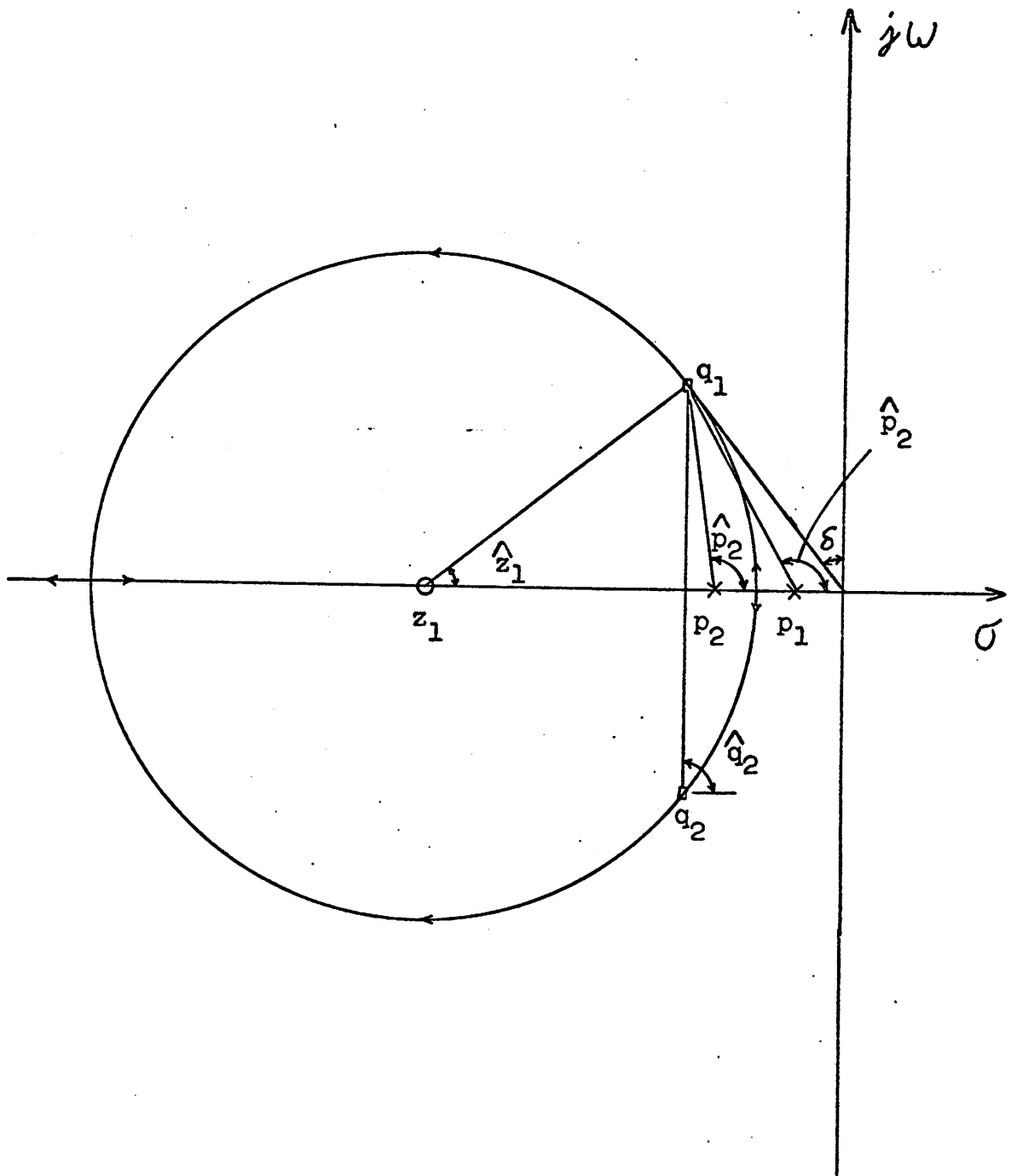


Fig. 11. Root locus of a two pole-one zero configuration

From Eqs. 91 and 92,  $z_1$  is given by

$$\hat{z}_1 = \delta = 0.573^\circ$$

and from Fig. 11,  $z_1$  is given by

$$z_1 = -\frac{|q_1|^2}{|\text{Re}(q_1)|} = -50.005 \times 10^6 \text{ rad/sec}$$

For convenience, assume  $p_1 = p_2 = p$ . Then from Fig. 11,  $p$  is given by

$$\begin{aligned} p &= z_1 + \frac{|q_1|}{\text{Tan } \delta} \\ &= -0.0025 \times 10^6 \text{ rad/sec} \end{aligned}$$

However, recall, from Fig. 4(a), that for the transistors chosen as typical,  $f_t = 600 \text{ MHz}$ . Consider the typical common emitter stage examined in Section I.C. When charge storage elements are included, analysis by computer indicates non-dominant poles due to these charge storage elements of the order of  $-2 \times 10^6 \text{ rad/sec}$ . This value is greater than the required value of  $z_1$ , and the excess phase resulting from these effects would surely distort the desired locus. Consequently, this configuration must be rejected.

It might appear possible to modify the above results by the addition of a second open-loop zero as shown in Fig. 12; however, it can be shown that such a placement of zeros does not alter the circular nature of the locus

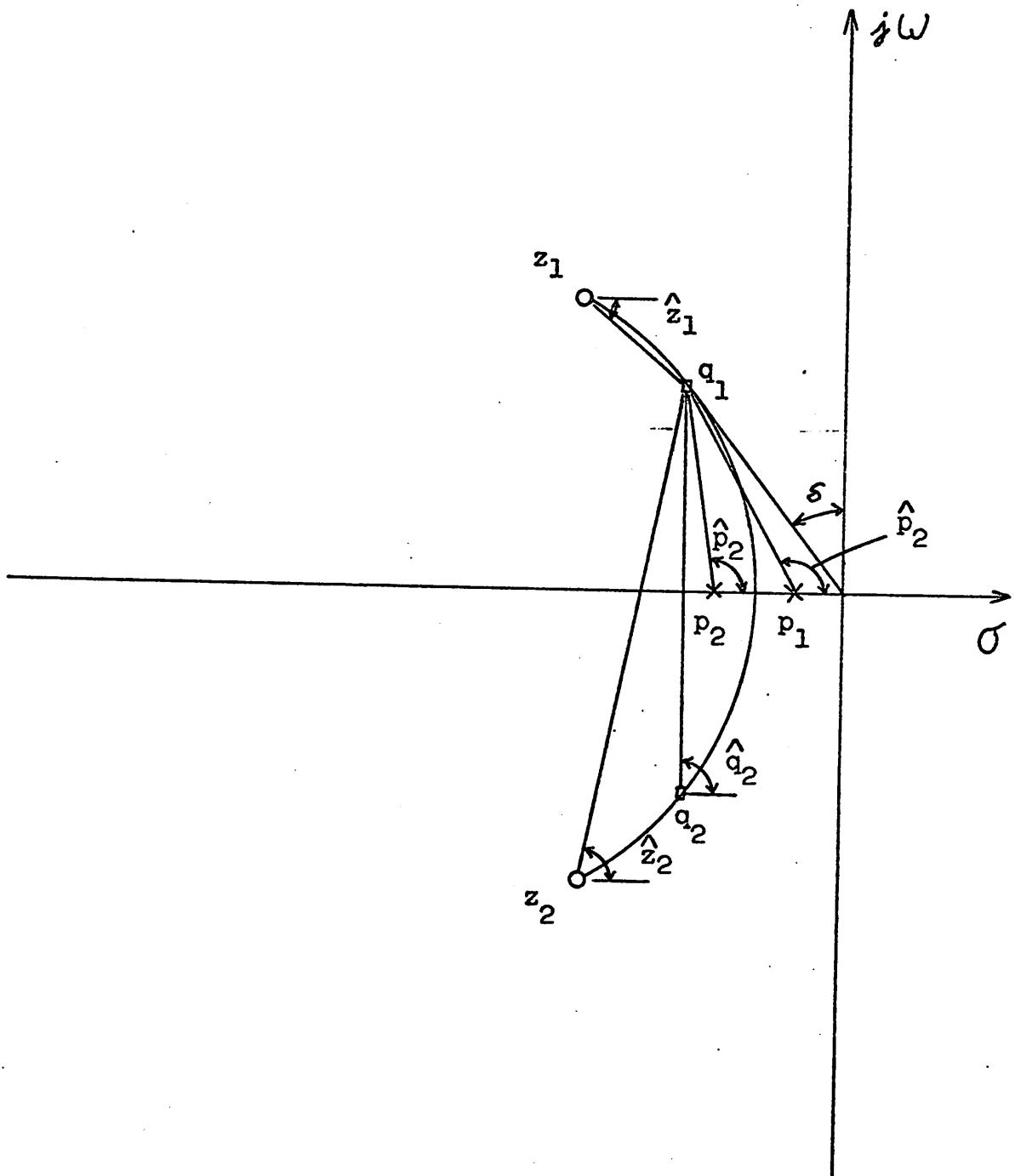


Fig. 12. Root locus of a two-pole, two-zero configuration.

previously considered. If it is assumed that the same values for  $q_{1,2}$  are required and that again  $p_1 = p_2 = p$ , the same value of  $p$  would be required as before. The largest passive base-diffused resistor which can readily be fabricated, keeping in mind reasonable amounts of chip area, power dissipation, and tolerance, is of the order of  $10\text{ k}\Omega$ . To realize the above value of  $p$ , one would require a corresponding value of capacitance of the order of  $40,000\text{ pf}$ . This is much larger than what one would normally like to use with integrated circuits. Further, conjugate complex zeros can be difficult to realize without introducing additional constraints on pole-zero locations.

As a third possibility, consider the type of pole-zero configuration depicted in Fig. 13. Based on intuition, it might appear to be possible to choose open-loop pole-zero locations such that the two phase conditions could be satisfied. However, at least one of the two open-loop poles  $p_1$  and  $p_2$  must still be greater than  $\text{Re}(q_{1,2})$ , again implying the need for excessively large capacitors. It is also possible that  $p_3$  will be of the same order of magnitude as the non-dominant excess phase effects due to charge storage in active devices.

As a final example, consider the pole-zero configuration of Fig. 14. This system is examined in detail in the next section, and consequently, no detailed justification for the shape of the locus is given now. It is apparent, however,

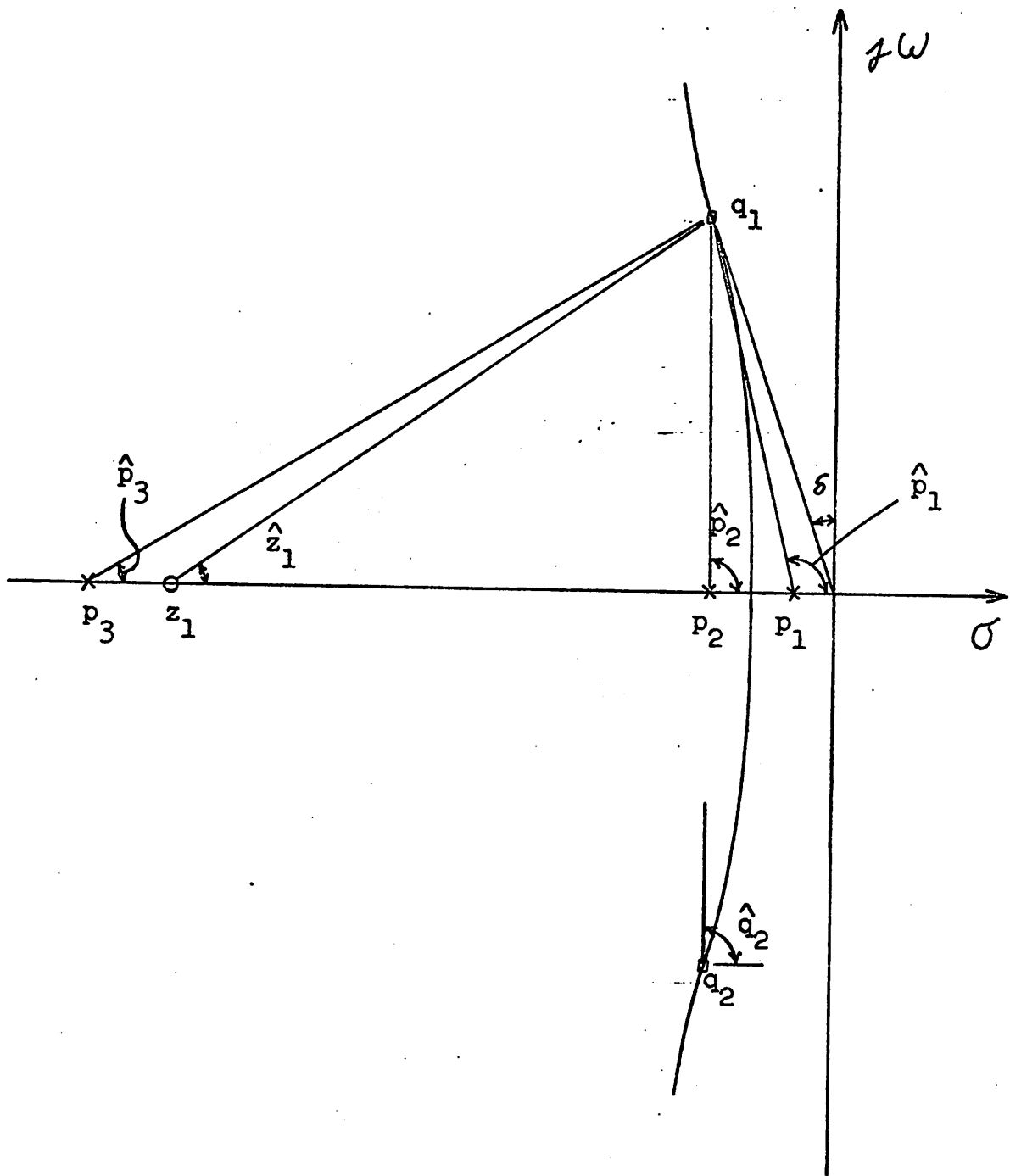


Fig. 13. Root locus of a three pole-one zero configuration.

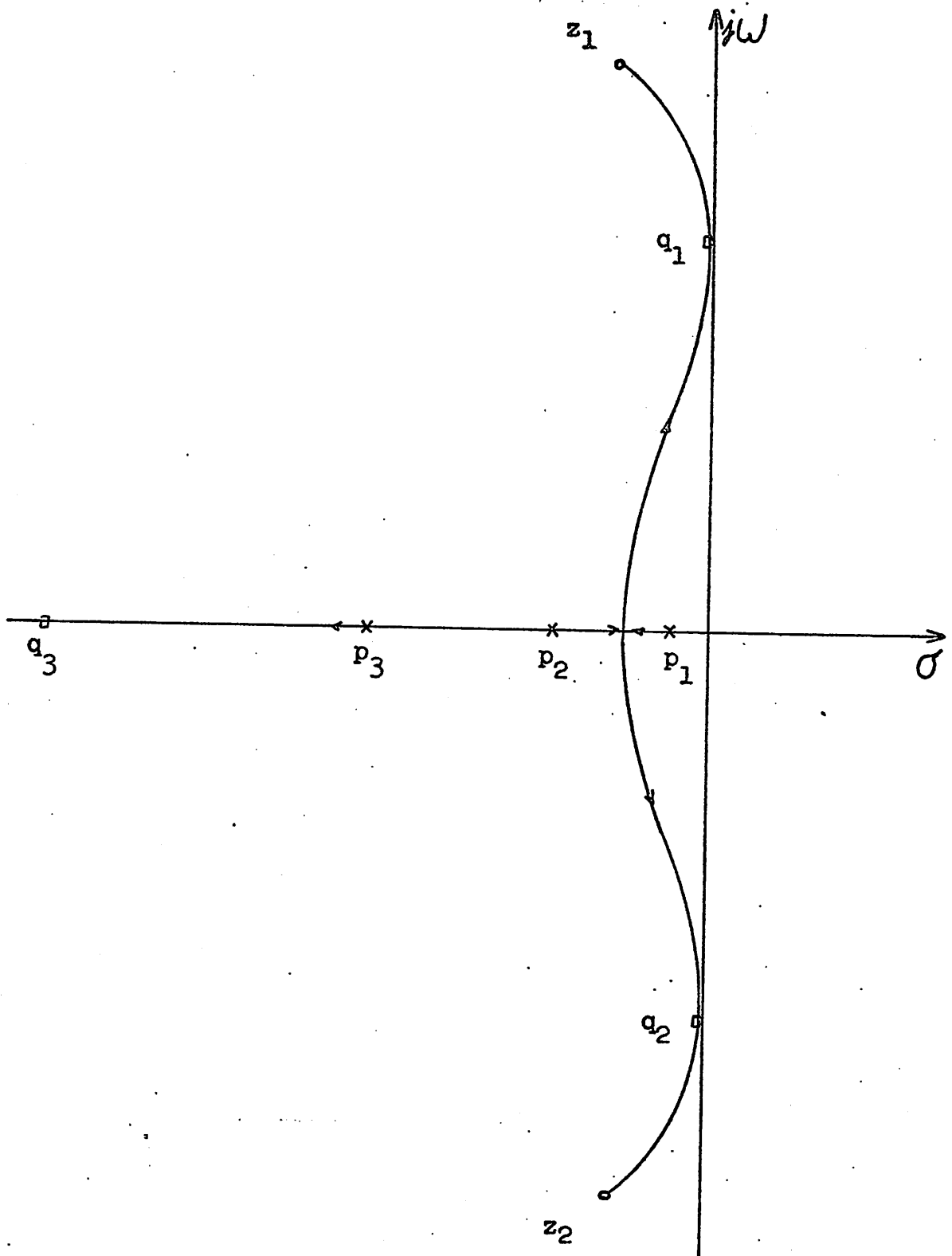


Fig. 14. Root locus of a three pole-two zero system.



that a pole-zero configuration such as this would allow the realization of reasonable high values of  $Q$  (narrow bandwidths) for a given center frequency,  $\omega_0$ , while not placing excessive demands on the RC products required to realize  $p_1$ ,  $p_2$ , and  $p_3$ .

### III. THE TEMPERATURE COMPENSATED SELECTIVE AMPLIFIER

In this section the single-loop feedback approach proposed by Gaash is considered. Attention is given to the influence on response and response sensitivity of second-order effects associated with monolithic diffused circuit realizations. Extensions are considered in order to encompass more realistic limitations on components and their temperature coefficients.

In the last section it was implied that an open-loop pole-zero configuration whose root locus is similar to that shown in Fig. 14 might be used to achieve desired center frequency, high selectivity, and response invariance. A zero-order realization of this system is shown in Fig. 15.  $R_L^I$  and  $R_L^{II}$  represent equivalent loads and are discussed shortly. The bridged-T network realizes the required complex conjugate zeros but introduces an additional constraint on the system. The transfer impedance of the bridged-T network is given by

$$z_{21}(s) = R_{BT} \frac{s^2 + (p_{01}(1+R_1/R_2)+p_{02})s + p_{01}p_{02}(1+R_1/R_{BT})}{s^2 + (p_{01}(1+R_1/R_2)+p_{02})s + p_{01}p_{02}} \quad (93)$$

where

$$p_{01} = 1/R_1 C_1 \quad (94a)$$

$$p_{02} = 1/R_2 C_2 \quad (94b)$$

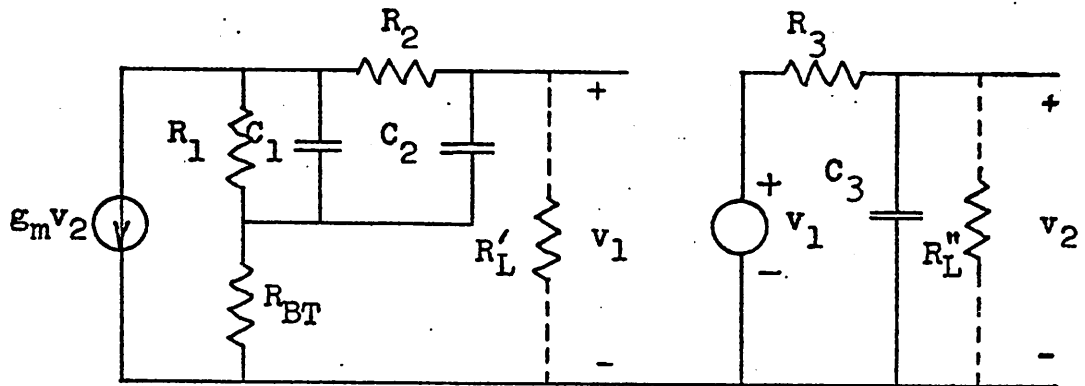


Fig. 15. Zero-order realization of a three pole-two zero system of the type shown in Fig. 14.

If the poles of  $z_{21}(s)$  are denoted  $p_1$  and  $p_2$ , the following constraint is placed on the zeros of  $z_{21}(s)$

$$\operatorname{Re}(z_{1,2}) = \frac{p_1 + p_2}{2} \quad (95)$$

There are no such constraints on  $\operatorname{Im}(z_{1,2})$ , which may be varied independently by varying  $R_{BT}$ . The third open-loop pole is determined by

$$p_3 = -1/R_3 C_3 \quad (96)$$

Four conditions must be satisfied for the simultaneous realization of specified response and response invariance. The first two conditions follow from Eq. 10 and are involved in the realization of the prescribed poles.

$$\left| T(s) \right|_{s=q_{1,2}} = 1 \quad (97a)$$

$$\operatorname{Arg} T(s) \Big|_{s=q_{1,2}} = \pi \quad (97b)$$

The second two conditions follow from Eqs. 66a and 67

$$\left| \begin{matrix} s^{q_1} & s^{T_0} \\ s^{T_0} & s^T \end{matrix} \right| = \left| \begin{matrix} s^{q_1} & s^e \\ s^e & s^T \end{matrix} \right| \quad (98a)$$

$$\operatorname{Arg} s^{q_1}_{T_0} = - \operatorname{Arg} s^{q_1}_e \quad (98b)$$

In general terms, the procedure followed will be to find open-loop pole and zero locations which satisfy the phase conditions, Eqs. 97b and 98b, subject to the added constraint on the real part of the complex zeros imposed by Eq. 95. Next, the required values of  $T_0$  and  $S_{T_0}^{q_1}$  will be chosen such that the magnitude conditions, Eqs. 97a and 98a, are satisfied.

For the configuration being considered,  $S_{T_0}^{q_1}$  can be written from Eq. 89 as

$$S_{T_0}^{q_1} = \frac{(q_1 - p_1)(q_1 - p_2)(q_1 - p_3)}{(q_1 - a_2)(q_1 - a_3)} \quad (99)$$

This equation can be written in terms of magnitude and phase as follows

$$S_{T_0}^{q_1} = \frac{|q_1 - p_1| |q_1 - p_2| |q_1 - p_3|}{|q_1 - a_2| |q_1 - a_3|} \quad (100a)$$

$$\begin{aligned} \text{Arg } S_{T_0}^{q_1} &= \hat{p}_1 + \hat{p}_2 + \hat{p}_3 - \hat{a}_2 - \hat{a}_3 \\ &= \hat{p}_1 + \hat{p}_2 + \hat{p}_3 - \pi/2 - \hat{a}_3 \end{aligned} \quad (100b)$$

The four conditions considered previously, Eqs. 97 and 98, can now be written

$$T_0 = \frac{|1 - a_1/p_1||1 - a_1/p_2||1 - a_1/p_3|}{|1 - a_1/z_1||1 - a_1/z_2|} \quad (101a)$$

or

$$K = \frac{|a_1 - p_1||a_1 - p_2||a_1 - p_3|}{|a_1 - z_1||a_1 - z_2|} \quad (101b)$$

$$\hat{z}_1 + \hat{z}_2 - \hat{p}_1 - \hat{p}_2 - \hat{p}_3 = \pi$$

and

$$\begin{matrix} S \\ T \end{matrix} T_0 = \frac{|a_1||a_1 - a_2||a_1 - a_3|}{|a_1 - p_1||a_1 - p_2||a_1 - p_3|} \begin{matrix} R \\ S \\ T \end{matrix} \quad (102a)$$

$$\hat{p}_1 + \hat{p}_2 + \hat{p}_3 - \hat{a}_3 = \pi + \delta \quad (102b)$$

where Eq. 31 has been used in deriving Eq. 102 and where it has been assumed that  $S_T^C = 0$ .

There are six degrees of design freedom associated with the realization of desired response and response invariance --  $p_1, p_2, p_3, \text{Im}(z_{1,2}), T_0$ , and  $S_T^{T_0}$ . Two of these are required by Eq. 101 to satisfy the magnitude and phase conditions such that  $q_1$  is a closed-loop pole. Two more degrees of freedom are required by Eq. 102 to insure that the tangent to the locus at the point  $q_1$  passes through the origin and that magnitudes are such that the desired cancellation of sensitivity vectors does occur. Two degrees of freedom

remain. Unfortunately, the obvious procedure of specifying  $T_0$  and  $S_T^0$  and then evaluating the remaining quantities  $p_1$ ,  $p_2$ ,  $p_3$ , and  $\text{Im}(z_{1,2})$  requires the simultaneous solution of Eqs. 101a, 101c, 102a, and 102b. The mathematics then becomes unduly complicated. An alternate procedure is to specify  $p_1$  and  $p_2$  and then solve for the required values of  $p_3$ ,  $\text{Im}(z_{1,2})$ ,  $T_0$ , and  $S_T^0$  and to then choose element values such that the original six quantities take on the specified values. This approach was followed by Gaash and is prompted by the fact that an iterative solution which converges rapidly is possible and is described below.

Prior to discussing this iterative design procedure, it will be necessary to establish two preliminary results. Consider two possible expansions for the numerator polynomial of  $D(s)$ .

$$s^3 - (q_1 + q_2 + q_3)s^2 + (q_1q_2 + q_2q_3 + q_3q_1)s - q_1q_2q_3 = 0 \quad (103)$$

$$s^3 - (p_1 + p_2 + p_3 - K)s^2 + (p_1p_2 + p_2p_3 + p_3p_1 - K(z_1 + z_2))s - p_1p_2p_3 + Kz_1z_2 = 0 \quad (104)$$

Corresponding coefficients of like powers must be equal; thus one can write

$$q_1 + q_2 + q_3 = p_1 + p_2 + p_3 - K \quad (105)$$

Next, it is necessary to consider the conditions imposed

on  $\text{Im}(z_{1,2})$  by the two phase conditions, Eqs. 101c and 102b. Combining these two equations, one obtains

$$\hat{z}_1 + \hat{z}_2 = \delta + \hat{q}_3 = \lambda \quad (106)$$

where for the present,  $q_3$  is assumed to be known and  $\lambda$  is a constant. Based on the assumed shape of the root locus of Fig. 14, assume that the following three conditions hold

$$\text{Im}(z_1) > \text{Im}(q_1) > 0 \quad (107)$$

$$\text{Re}(z_1) < \text{Re}(q_1) < 0 \quad (108)$$

$$z_2 = \overline{z_1} \quad (109)$$

By defining the following variables

$$y_1 = \text{Im}(z_1) - \text{Im}(q_1) \quad (110a)$$

$$y_2 = \text{Im}(z_1) + \text{Im}(q_2) \quad (110b)$$

$$x = \text{Re}(q_1) - \text{Re}(z_1) \quad (110c)$$

one can write  $z_1$  and  $z_2$  in the following manner

$$\hat{z}_1 = -\tan^{-1}(y_1/x) \quad (111a)$$

$$\hat{z}_2 = \tan^{-1}(y_2/x) \quad (111b)$$

Thus from Eq. 106,  $\lambda$  can be written



$$\lambda = \tan^{-1} (y_2/x) - \tan^{-1} (y_1/x) \quad (112)$$

Now define  $N = \tan \lambda$ . Then the following identity holds

$$N = \frac{y_2/x - y_1/x}{1 + (y_2/x)(y_1/x)} = \tan \lambda \quad (113)$$

or

$$x^2 N + y_2 y_1 N = x(y_2 - y_1) \quad (114)$$

Substituting from Eq. 110 and rearranging terms, one obtains

$$\text{Im}^2(z_1) = (\text{Re}(q_1) - \text{Re}(z_1))^2 \left[ \frac{2\text{Im}(q_1)}{\tan \lambda (\text{Re}(q_1) - \text{Re}(z_1))} - 1 \right] + \text{Im}^2(q_1) \quad (115)$$

It is now possible to formulate a design procedure for determining the required open-loop singularities, loop gain, and gain sensitivity. This design procedure is presented in Table 4. It may be carried out graphically using constant phase loci<sup>20</sup> as was proposed by Gaash<sup>7</sup> or more easily and accurately on a digital computer. Note that usually a knowledge of  $q_{1,2}$  and of the general shape of the locus are sufficient to suggest reasonable values for  $p_1$  and  $p_2$ ; however, this will be discussed in more detail shortly.

First, by way of example, consider the design and realization originally proposed by Gaash.<sup>7,8</sup> The desired center

Table 4

Iterative Design Procedure

- 1) Assume  $q_1$  and  $q_2 = \bar{q}_1$  are specified.
- 2) Choose  $p_1$  and  $p_2$ .
- 3) From Eq. 95, determine  $\text{Re}(z_{1,2})$ .
- 4) Find  $\hat{p}_1$  and  $\hat{p}_2$ .
- 5) From Eq. 102b, find  $\hat{p}_3 - \hat{q}_3$ .
- 6) Choose a trial  $p_3$ .
- 7) Evaluate  $\hat{p}_3$ ,  $\hat{q}_3$ , and  $q_3$ .
- 8) Determine  $\text{Im}(z_{1,2})$  from Eq. 115.
- 9) Determine  $K$  from Eq. 101b.
- 10) From Eq. 105, find the required value of  $(p_3 - q_3)$  and compare this with the actual value.
  - a) If the required value is greater than the actual value, shift  $p_3$  to the left (increase  $|p_3|$ ).
  - b) If the required value is less than the actual value, shift  $p_3$  to the right (decrease  $|p_3|$ ).
  - c) If the values are equal, this stage of the design is complete.
- 11) Determine the required value of  $T_0$  from Eq. 101a.
- 12) Determine the required value of  $S_T^{T_0}$  from Eq. 102a.

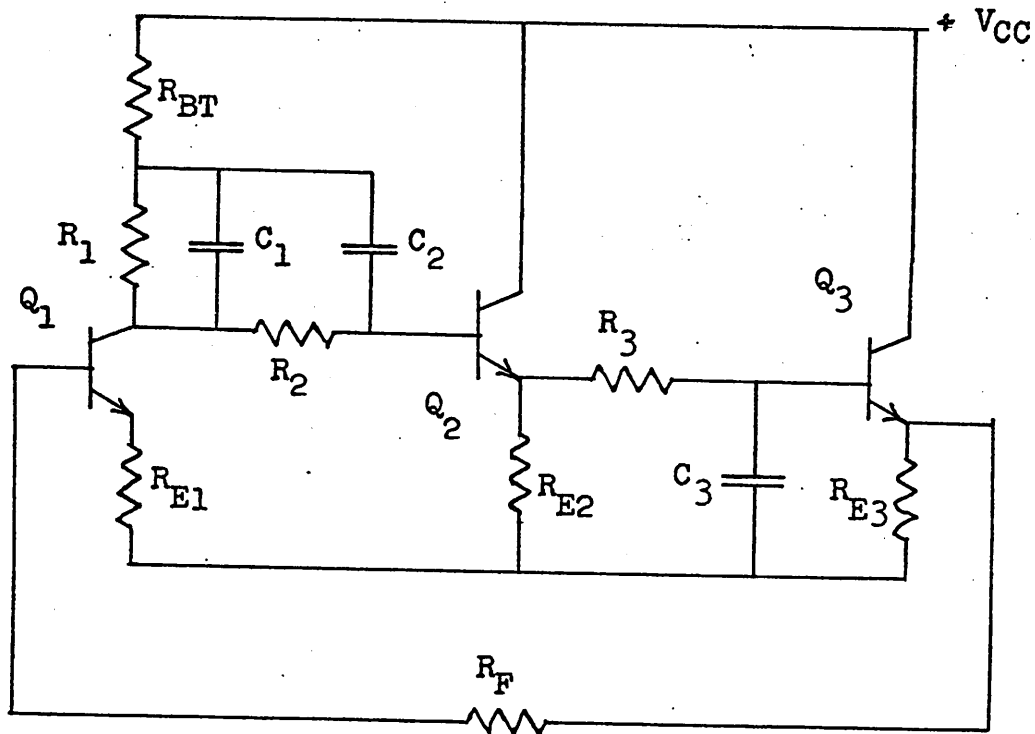
frequency was assumed to be 79.5 kHz. with a selectivity of  $Q = 50$ . The design values proposed by Gaash are presented below in the first column of Table 5. In the second column are the design values as determined by the design procedure of Table 4 when implemented on a computer. A comparison indicates reasonable agreement between the two methods. It is important to note that in arriving at these design values, Gaash assumed  $S_T^R = 0.36$  ( $\gamma_T^R = 1200 \text{ ppm}/^\circ\text{C}$  at  $300^\circ\text{K}$ ) with  $S_T^C = 0$ .<sup>7</sup> Based on the requirements of Table 5, the realization of Fig. 16 was proposed by Gaash. It is apparent that the basic amplifier is the same shunt-shunt feedback configuration considered in Section I.D with the addition of the bridged-T network. As before, the collector bias currents indicated closely approximate measured values. In the following discussion, a familiarity with this circuits basic characteristics is assumed.

The results of a computer analysis of the zero-order realization of Fig. 15 with the appropriate design values for  $R_1$ ,  $C_1$ ,  $R_2$ ,  $C_2$ ,  $R_{BT}$ ,  $R_3$ , and  $C_3$  taken from the circuit of Fig. 16 are presented in the first column of Table 6. Note that the dependent, voltage-controlled current source in Fig. 15 cannot be identified with the transconductance or related to the collector current of a specific transistor in Fig. 16. It is strictly an idealization, and  $g_m$  was chosen such that  $T_0 = g_m(R_1 + R_{BT}) = 70$  in agreement with Gaash's required design value. Further, in considering

Table 5

Temperature Compensated Single-Loop Feedback Selective Amplifier Design Requirements Proposed by Gaash.  
 (Frequency in rad/sec x 10<sup>6</sup>. Sensitivity in ppm/°C.)

	Graphical	Analytical
$q_{1,2}$	$-0.00500 \pm j0.500$	$-0.00500 \pm j0.500$
$\omega_0$	0.500	0.500
BW	0.0100	0.0100
Q	50.0	50.0
$P_{01}$	0.100	0.100
$P_{02}$	0.100	0.100
$P_1$	-0.0500	-0.0500
$P_2$	-0.200	-0.200
$P_3$	-0.440	-0.441
$z_{1,2}$	$-0.125 \pm j0.725$	$-0.125 \pm j0.725$
$-\gamma_T^e$	-1200	-1200
$T_0$	70.0	69.8
$\gamma_T^{T_0}$	+4350	+4500



$R_1 = 5 \text{ k}\Omega$	$R_3 = 3 \text{ k}\Omega$	$R_F = 5 \text{ k}\Omega$
$C_1 = 2000 \text{ pF}$	$C_3 = 750 \text{ pF}$	$V_{CC} = 12.5 \text{ V}$
$R_2 = 10 \text{ k}\Omega$	$R_{E1} = 10 \Omega$	$I_{C1} = 2.0 \text{ mA}$
$C_2 = 1000 \text{ pF}$	$R_{E2} = 3 \text{ k}\Omega$	$I_{C2} = 0.5 \text{ mA}$
$R_{BT} = 95 \Omega$	$R_{E3} = 3 \text{ k}\Omega$	$I_{C3} = 0.25 \text{ mA}$

Fig. 16. Single-loop feedback selective amplifier realization proposed by A. A. Gaash.

Table 6

Response and Response Sensitivity of the Original  
Gaash Single Loop Feedback Frequency Selective Amplifier.  
(Frequency in rad/sec  $\times 10^6$ . Sensitivity in ppm/ $^{\circ}$ C.)

Open Loop	Zero-Order	First-Order	Second-Order
$p_1$	-0.0500	-0.0519	-0.0565
$\gamma_T^{p_1}$	-1192	-1420	-1740
$p_2$	-0.200	-0.200	-0.206
$\gamma_T^{p_2}$	-1193	-1200	-1450
$p_3$	-0.444	-0.447	-0.448
$\gamma_T^{p_3}$	-1194	-1380	-1380
$z_{1,2}$	$-0.125 \pm j0.722$	$-0.125 \pm j0.722$	$-0.125 \pm j0.722$
$\gamma_T^{\text{Re}(z_1)}$	-1193	-1193	-1193
$\gamma_T^{\text{Im}(z_1)}$	-1193	-1193	-1193
$T_0$	70.0	62.0	51.8
$\gamma_T^{T_0}$	+4350	+4350	+4810

Closed Loop	Zero-Order	First-Order	Second-Order
$q_{1,2}$	$-0.00636 \pm j0.500$	$-0.00734 \pm j0.489$	$-0.00820 \pm j0.481$
$q_3$	-1.26	-1.22	-1.21
$z_{1,2}$	$-0.125 \pm j0.722$	$-0.127 \pm j0.719$	$-0.127 \pm j0.719$
$\omega_0$	0.500	0.489	0.481
$\gamma_T^{\omega_0}$	-63.5	-126	-121
BW	0.0127	0.0147	0.0164
$\gamma_T^{\text{BW}}$	+515	-3900	-7800
Q	39.2	33.3	29.3
$\gamma_T^Q$	-568	+3770	+7680

response as a function of temperature,  $g_m$  was varied so as to simulate a sensitivity of  $T_0$  of 4350 ppm/°C also in agreement with Gaash's required design value. The results of a first-order analysis of the circuit of Fig. 16, where the reduced hybrid-pi model of Fig. 4(b) was used, are given in the second column of Table 6. Finally, in the third column are the results of a second-order analysis where the more complete hybrid-pi model of Fig. 4(a) was considered. It can be seen that even for the zero-order realization, the response is not quite that desired as  $Q$  is only 39.2. Examining the open loop response, it is seen that  $\text{Im}(z_{1,2})$  and  $p_3$  do not agree with the required values proposed by Gaash. Also, the sensitivities of the open-loop poles and zeros reflect the fact that differential quantities have been approximated by larger increments (i.e.  $dT = \Delta T = 5^\circ\text{C}$ ). Both the response and its sensitivity become progressively worse as the first and second-order models are considered.

Slight adjustments of  $R_{BT}$  and  $C_3$  to 94.1  $\Omega$  and 755.7 pF., respectively, are sufficient to bring about the desired closed-loop response for the zero-order realization as indicated by the results of Table 7. Here, also, for the zero-order realization,  $g_m$  and its temperature sensitivity were chosen so as to reflect the design requirements of the second column of Table 5 rather than those proposed by Gaash as given in the first column. Note that for the zero-order realization, all open-loop requirements are satisfied

to three place accuracy with the exception of the temperature sensitivities of the open-loop poles and zeros, yet the sensitivity of bandwidth is relatively large. This point will be brought out further shortly. Considering the results of the first and second-order analyses, it is also seen that what little improvement in performance is achieved in terms of bandwidth and center frequency is more than offset by the corresponding increase in sensitivity.

If the open-loop results of Table 7 for the first-order analysis are examined, it is apparent that several parameters do not agree well with their corresponding zero-order values or the required values as specified in Table 5. Consider the shift in  $p_1$  and  $p_2$  from the zero-order to the first-order realization. This is the result of a finite load introduced across the output of the bridged-T network. Let  $R'_L$  denote the equivalent load seen by the network as indicated in Fig. 15. It represents the driving point resistance presented by the first emitter-follower. The expression for the transimpedance  $z_{21}(s)$  of the bridged-T network becomes

$$z_{21}(s) = \frac{R_{BT}R'_L s^2 + p_{o1}\left(1+\frac{R_1}{R_2}\right)+p_{o2} s + p_{o1}p_{o2}\left(1+\frac{R_1}{R_{BT}}\right)}{R_{BT}+R'_L s^2 + p_{o1}\left(1+\frac{R_1}{R_2}\right)+p_{o2}\left(1+\frac{R_2}{R_{BT}+R'_L}\right) s + p_{o1}p_{o2}\left(1+\frac{R_1+R_2}{R_{BT}+R'_L}\right)} \quad (116)$$



Table 7

Response and Response Sensitivity of the Corrected Zero-Order-Design Selective Amplifier where  $R_{BT} = 94.1\Omega$  and  $C_3 = 755.7\text{pf}$ . (Frequency in rad/sec  $\times 10^6$ . Sensitivity in ppm/ $^{\circ}\text{C}$ .)

Open Loop	Zero-Order	First-Order	Second-Order
$p_1$	-0.0500	-0.0519	-0.0565
$\gamma_T^{p_1}$	-1191	-1420	-1740
$p_2$	-0.200	-0.200	-0.206
$\gamma_T^{p_2}$	-1193	-1200	-1450
$p_3$	-0.441	-0.444	-0.444
$\gamma_T^{p_3}$	-1193	-1380	-1380
$z_{1,2}$	$-0.125 \pm j0.725$	$-0.125 \pm j0.725$	$-0.125 \pm j0.725$
$\gamma_T^{\text{Re}(z_1)}$	-1193	-1193	-1193
$\gamma_T^{\text{Im}(z_1)}$	-1193	-1193	-1193
$T_0$	69.8	62.0	51.8
$\gamma_T^{T_0}$	+4500	+4350	+4810

Closed Loop	Zero-Order	First-Order	Second-Order
$q_{1,2}$	$-0.00503 \pm j0.500$	$-0.00607 \pm j0.490$	$-0.00698 \pm j0.481$
$q_3$	-1.25	-1.21	-1.20
$z_{1,2}$	$-0.125 \pm j0.725$	$-0.128 \pm j0.727$	$-0.128 \pm j0.727$
$\omega_0$	0.500	0.490	0.481
$\gamma_T^{\omega_0}$	-17.5	-121	-116
BW	0.0101	0.0121	0.0140
$\gamma_T^{\text{BW}}$	+418	-4900	-9900
Q	49.7	40.4	34.5
$\gamma_T^Q$	-435	+4780	+9780

where  $p_{o1}$  and  $p_{o2}$  are defined as before. It is seen that the loading does not affect the zeros of  $z_{21}(s)$ . The loading does, however, introduce  $R_{BT}$  into the denominator of the expression for  $z_{21}(s)$ . It might appear that this would preclude one from adjusting  $\text{Im}(z_{1,2})$  independently of  $p_1$  and  $p_2$ . Fortunately, in the case being considered,  $R_{BT}$  is negligible with respect to  $R'_L$  which is of the order of  $300 \text{ k}\Omega$ .  $R_{BT}$  can thus be neglected.

In the original work of Gaash, losses through the emitter followers were assumed negligible. Note that the common emitter stage (transistor  $Q_1$ ) of the realization of Fig. 16 is nearly the same as that considered in Section I.D which has a current gain of approximately -69. If this value is compared with that of the loop gain from Table 7, it becomes apparent that the above mentioned losses are not negligible. If Eqs. 46 and 47 are considered, it is seen that this problem can be corrected while preserving the proper gain sensitivity by varying  $R_F$  and  $R_{E1}$ . The required values and the results of a first and second-order analysis of this gain corrected circuit are presented in Table 8.

Notice that  $Q$  is relatively unaffected by this correction. This leads to the consideration of the tolerance problem associated with  $R_{BT}$ . In Fig. 17 is a plot of  $\text{Re}(q_{1,2})$ ,  $\text{Im}(q_{1,2})$  and  $Q_{(\text{unloaded})}$  as a function of  $R_{BT}$  corresponding to the zero-order realization of Fig. 15. Also shown (dashed line) is the curve for  $Q_{(\text{loaded})}$ , that is, for

Table 8

Response and Response Sensitivity for Gain Corrected Design where  $R_{E1} = 6\Omega$ ,  $R_F = 4.6\text{ k}\Omega$ ,  $R_{BT} = 94.1\Omega$ , and  $C_3 = 755.7\text{ pf}$ . (Frequency in rad/sec  $\times 10^6$ . Sensitivity in ppm/ $^\circ\text{C}$ .)

Open Loop	First-Order	Second-Order
$p_1$	-0.0519	-0.0567
$\gamma_{T}^{p_1}$	-1420	-1740
$p_2$	-0.200	-0.206
$\gamma_{T}^{p_2}$	-1200	-1450
$p_3$	-0.444	-0.445
$\gamma_{T}^{p_3}$	-1380	-1380
$z_{1,2}$	$-0.125 \pm j0.725$	$-0.125 \pm j0.725$
$\gamma_{T}^{\text{Re}(z_1)}$	-1193	-1193
$\gamma_{T}^{\text{Im}(z_1)}$	-1193	-1193
$T_0$	69.56	57.81
$\gamma_{T}^{T_0}$	+4450	+4690

Closed Loop	First-Order	Second-Order
$q_{1,2}$	$-0.00614 \pm j0.505$	$-0.00669 \pm j0.496$
$q_3$	-1.27	-1.27
$z_{1,2}$	$-0.128 \pm j0.727$	$-0.128 \pm j0.727$
$\omega_0$	0.505	0.496
$\gamma_{T}^{\omega_0}$	-132	-124
BW	0.0123	0.0134
$\gamma_{T}^{\text{BW}}$	-1700	-7650
Q	41.1	37.1
$\gamma_{T}^Q$	+1560	+7525

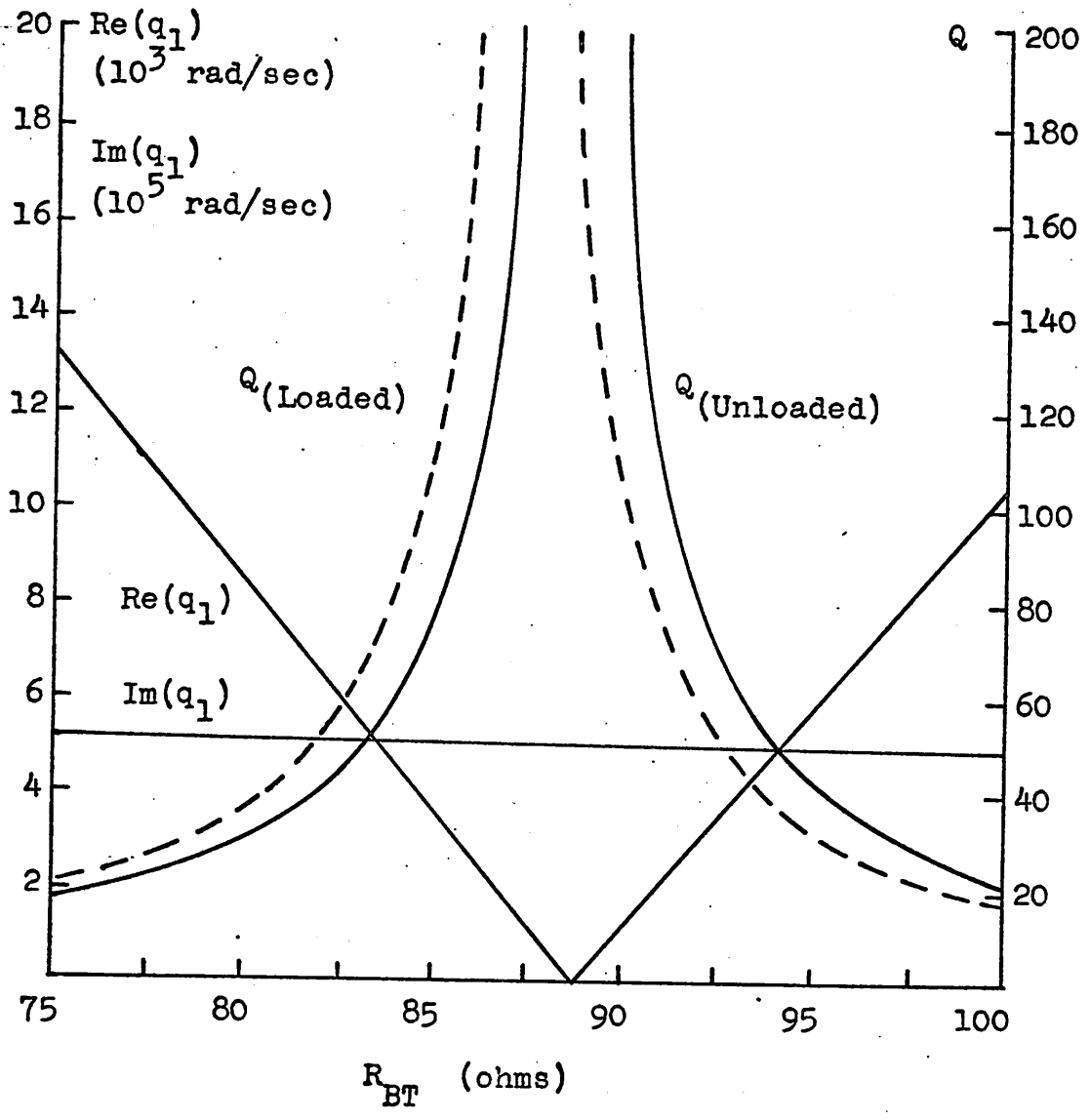


Fig. 17. Effect on  $Q$  of  $R_{BT}$  and loading.

$Q$  where a 300 k $\Omega$  load has been placed across the output of the bridged-T network. Clearly, the sharp dependence of  $Q$  on  $R_{BT}$  as well as the dependence of  $Q$  on loading could lead to difficulties.

In an effort to surmount these problems, consider the following optimization scheme. Rather than redesigning the circuit and accounting for the loading problem discussed above, use the values of  $p_1$  and  $p_2$  from Table 8 and the value of  $\text{Re}(z_{1,2})$  rather than Eq. 95 in the design procedure of Table 4. Loading effects are then taken into account. This will result in new required values of  $p_3$ ,  $\text{Im}(z_{1,2})$ ,  $T_0$ , and  $S_T^{T_0}$ . The new required value of  $p_3$  can be realized by the proper choice of  $C_3$ . The new required values of  $T_0$  and  $S_T^{T_0}$  can be realized by the proper choice of  $R_F$  and  $R_{E1}$ . Finally, the new required value of  $\text{Im}(z_{1,2})$  can be realized by the proper choice of  $R_{BT}$ . Note that each of these three adjustments can be made relatively independently of the other two as interaction is negligible. Such a procedure results in the revised design requirements and element changes given in Table 9. The resulting performance is characterized in Table 10. It is seen that at least to first-order the response is that desired.

The problem of the large sensitivity of bandwidth ( $\text{Re}(q_{1,2})$ ) has not been resolved. The only noticeable remaining deviations from specified design values are in the sensitivities of the open-loop poles  $p_1$  and  $p_3$ . Recall

Table 9

Modified Design Requirements and New Element Values Required to Compensate for the Effects Due to Finite Active Loads. (Frequency in rad/sec x 10<sup>6</sup>. Sensitivity in ppm/°C.)

Modified Design Requirements	
$p_1 = -0.0519$	$q_{1,2} = -0.00500 \pm j0.500$
$p_2 = -0.200$	$\omega_o = 0.500$
$p_3 = -0.437$	$BW = 0.0100$
$z_{1,2} = -0.125 \pm j0.725$	$Q = 50.0$
$T_o = 67.72$	$\gamma_T^{T_o} = +4511$

New Element Values	
$R_{E1} = 6.3 \Omega$	$R_{BT} = 94.1 \Omega$
$R_F = 4.75 \text{ k}\Omega$	$C_3 = 768.0 \text{ pf.}$

however that the fundamental assumption upon which all of the foregoing design procedure is based is that all dominant open-loop poles and zeros have the same sensitivity with respect to temperature.

The departure of  $S_T^{p_1}$  and  $S_T^{p_3}$  from the desired uniform sensitivity of 0.36 (1200 ppm/°C at 300°K) can be attributed to the increased temperature sensitivity due to  $B_0$  of the active load presented to the bridged-T network and to the  $R_3$ - $C_3$  combination by the two emitter followers. The effect of these deviations can be demonstrated as follows. From Eq. 15, one obtains

$$dq_1 = S_{T_0}^{q_1} \frac{dT_0}{T_0} + S_{T_0}^{q_1} \sum_e \frac{q_1}{q_1 - p_e} \frac{dp_e}{p_e} - S_{T_0}^{q_1} \sum_k \frac{q_1}{q_1 - z_k} \frac{dz_k}{z_k} \quad (117)$$

From Eq. 35,  $dT_0/T_0$  can be related to  $dT/T$  by  $S_T^{T_0}$ . Assume that based on some design, a required value of  $S_T^{T_0}$ , here denoted  $\hat{S}_T^{T_0}$ , is known. Let  $\Delta S_T^{T_0}$  denote the error between the actual value and the required value

$$\Delta S_T^{T_0} = S_T^{T_0} - \hat{S}_T^{T_0} \quad (118)$$

Similarly, from Eq. 9, one can write

$$\frac{dp_e}{p_e} = S_T^{p_e} \frac{dT}{T} \quad (119a)$$

$$\frac{dz_k}{z_k} = S_T^{z_k} \frac{dT}{T} \quad (119b)$$

Again assume that required values, denoted  $\hat{S}_T^{p_e}$  and  $\hat{S}_T^{z_k}$ , of  $S_T^{p_e}$  and  $S_T^{z_k}$  are known such that

$$\hat{S}_T^{p_e} = \hat{S}_T^{z_k} = -(S_T^R + S_T^C) \quad (120)$$

Let  $\Delta S_T^{p_e}$  and  $\Delta S_T^{z_k}$  denote the errors between the actual values and the required values

$$\Delta S_T^{p_e} = S_T^{p_e} - \hat{S}_T^{p_e} \quad (121a)$$

$$\Delta S_T^{z_k} = S_T^{z_k} - \hat{S}_T^{z_k} \quad (121b)$$

Then Eq. 117 may be written

$$dq_1 = S_{T_0}^{q_1} \left[ (\hat{S}_T^{T_0} + \Delta \hat{S}_T^{T_0}) + \sum_e \frac{q_1}{q_1 - p_e} (\hat{S}_T^{p_e} + \Delta S_T^{p_e}) - \sum_k \frac{q_1}{q_1 - z_k} (\hat{S}_T^{z_k} + \Delta S_T^{z_k}) \right] \frac{dT}{T} \quad (122)$$

Now assume that for the required values first-order compensation is achieved

$$S_{T_0}^{q_1} \hat{S}_T^{T_0} + q_1 S_{T_0}^{q_1} \left[ \sum_e \frac{1}{q_1 - p_e} \hat{S}_T^{p_e} - \sum_k \frac{1}{q_1 - z_k} \hat{S}_T^{z_k} \right] = 0 \quad (123)$$



Then Eq. 122 reduces to

$$dq_1 = \left[ s_{T_0}^{q_1} \Delta s_T^{T_0} + q_1 s_{T_0}^{q_1} \left( \sum_e \frac{1}{e^{q_1 - p_e}} \Delta s_T^{p_e} - \sum_k \frac{1}{q_1 - z_k} \Delta s_T^{z_k} \right) \right] \frac{dT}{T} \quad (124)$$

Now from Fig. 10 and Eqs. 16 and 88, one can write

$$s_{T_0}^{q_1} = \left| s_{T_0}^{q_1} \right| e^{j(\pi/2 + \delta)} = j \left| s_{T_0}^{q_1} \right| e^{j\delta} \quad (125)$$

and

$$q_1 s_{T_0}^{q_1} = \left| q_1 \left| s_{T_0}^{q_1} \right| \right| e^{j(\pi + 2\delta)} = - \left| q_1 \left| s_{T_0}^{q_1} \right| \right| e^{j2\delta} \quad (126)$$

For a high  $Q$  ( $\geq 30$ ) circuit,  $\delta$  is small ( $< 1^\circ$ ) and these equations may be approximated by

$$s_{T_0}^{q_1} \approx j \left| s_{T_0}^{q_1} \right| \quad (127)$$

$$-q_1 s_{T_0}^{q_1} \approx - \left| q_1 \left| s_{T_0}^{q_1} \right| \right| \quad (128)$$

Eq. 124 may now be approximated by

$$dq_1 \approx \left[ j \left| s_{T_0}^{q_1} \right| \Delta s_T^{T_0} - \left| q_1 \left| s_{T_0}^{q_1} \right| \right| \left( \sum_e \frac{1}{e^{q_1 - p_e}} \Delta s_T^{p_e} - \sum_k \frac{1}{q_1 - z_k} \Delta s_T^{z_k} \right) \right] \frac{dT}{T} \quad (129)$$

Now from Eq. 60, the sensitivity of center frequency,  $\omega_0$ , is given by

$$S_{T}^{\omega} \approx S_{T}^{\text{Im}(q_1)}$$

$$\approx \frac{\partial \text{Im}(q_1) / \text{Im}(q_1)}{\partial T / T}$$

$$\approx \frac{\text{Im}(\partial q_1) / \text{Im}(q_1)}{\partial T / T}$$

$$\approx \frac{|S_{T_0}^{q_1}| \Delta S_T^{T_0}}{\text{Im}(q_1)} - \frac{|q_1| |S_{T_0}^{q_1}|}{\text{Im}(q_1)} \text{Im} \left[ \sum \frac{1}{e^{q_1 - p_e}} \Delta S_T^{p_e} - \sum_k \frac{1}{q_1 - z_k} \Delta S_T^{z_k} \right]$$

$$\approx \left| S_{T_0}^{q_1} \right| \left[ \frac{\Delta S_T^{T_0}}{\text{Im}(q_1)} - \text{Im} \left( \sum \frac{1}{e^{q_1 - p_e}} \Delta S_T^{p_e} - \sum_k \frac{1}{q_1 - z_k} \Delta S_T^{z_k} \right) \right] \quad (130)$$

where for a high Q situation, the approximation

$$\text{Im}(q_1) \approx |q_1|$$

has been used.

Similarly from Eq. 63, the sensitivity of bandwidth, BW, is given by

$$S_{T}^{\text{BW}} \approx S_{T}^{\text{Re}(q_1)}$$

$$\approx \frac{\partial \text{Re}(q_1) / \text{Re}(q_1)}{\partial T / T}$$

$$\begin{aligned}
& \approx \frac{\operatorname{Re}(\partial q_1) / \operatorname{Re}(q_1)}{\partial T / T} \\
& \approx -\frac{|q_1| \left| \frac{q_1}{s_{T_0}} \right|}{\operatorname{Re}(q_1)} \operatorname{Re} \left[ \sum_e \frac{1}{q_1 - p_e} \Delta s_T^{p_e} - \sum_k \frac{1}{q_1 - z_k} \Delta s_T^{z_k} \right] \\
& \approx 2Q \left| \frac{q_1}{s_{T_0}} \right| \operatorname{Re} \left[ \sum_e \frac{1}{q_1 - p_e} \Delta s_T^{p_e} - \sum_k \frac{1}{q_1 - z_k} \Delta s_T^{z_k} \right] \quad (131)
\end{aligned}$$

The important point to notice here is the appearance of the factor  $2Q$  in the expression for the sensitivity of bandwidth.

For the optimized first-order design considered above, the deviations in the sensitivities of the open-loop parameters are

$$\Delta s_T^{p_2} \approx \Delta s_T^{z_{1,2}} \approx \Delta s_T^{T_0} \approx 0$$

and

$$\Delta s_T^{p_1} \approx -0.066$$

$$\Delta s_T^{p_3} \approx -0.054$$

For the assumed first-order compensation,  $\left| \frac{q_1}{s_{T_0}} \right|$  can be approximated by

$$\left| \frac{q_1}{s_{T_0}} \right| \approx |q_1| \left( \frac{s_T^R}{s_T^{T_0}} \right) \approx 0.133$$

where  $S_T^C = 0$ . Using these values and the values for  $p_1$ ,  $p_3$ , and  $q_1$  from Table 10, one obtains from Eqs. 130 and 131

$$S_T^{\omega_0} \approx -(0.133) \operatorname{Im} \left( \frac{-0.066}{q_1 - p_1} + \frac{-0.054}{q_1 - p_3} \right)$$

$$\approx -(0.0176 + 0.0082)$$

$$\approx -0.0258$$

$$S_T^{BW} \approx 2(50)(0.133) \operatorname{Re} \left( \frac{-0.066}{q_1 - p_1} + \frac{-0.054}{q_1 - p_3} \right)$$

$$\approx -(0.165 + 0.708)$$

$$\approx -0.873$$

At 300°K,

$$\gamma_T^{\omega_0} \approx -86 \text{ ppm/ } ^\circ\text{C}$$

$$\gamma_T^{BW} \approx -2910 \text{ ppm/ } ^\circ\text{C}$$

These values agree well with the actual sensitivities found for center frequency and bandwidth as given in Table 10.

Notice the relative magnitudes of the contributions to the sensitivity of bandwidth from the poles  $p_1$  and  $p_2$ . This results from the fact that  $|p_1|$ , and thus  $\operatorname{Re}(q_1 - p_1)$ , is small with respect to  $|q_1| \approx \omega_0$  while  $|p_3|$  is of the same order of magnitude. This observation will be referred to when exten-

sions of Gaash's are considered.

As a final point prior to discussing the results of the second-order analyses, notice the slight shift in the locations of the zeros in going from open to closed-loop. It can be shown that this is due to feed-forward through  $R_F$  as follows. Assume temporarily that the input node is the collector of  $Q_1$  rather than the base. The resulting circuit is still recognized as a shunt-shunt configuration. For a first order, small-signal analysis, however, the controlled source of the reduced hybrid-pi model is unilateral, and feed-forward is eliminated. Under such conditions, no shift in zero locations is observed yet the closed-loop poles are found to be identical with those observed in generating Tables 6, 7, 8, and 10. Based on these results, the shift in zero locations will be ignored.

If the results of the second-order analyses are examined, three effects are quite noticeable. First, additional loading results in a larger deviation of  $p_1$  from its predicted value. Second, the sensitivities of the open-loop poles are significantly larger. Finally, loop gain is reduced further by losses associated with  $r_x$ ,  $r_\mu$ ,  $r_o$ , and  $r_c'$ . As a result, the closed-loop response is not that desired, while the sensitivity of bandwidth is much worse.

Before attempting a sensitivity analysis such as that carried out above for the first-order response, consider the results obtained by following an optimization procedure

such as was done for the first-order analysis. Values of the open-loop poles  $p_1$  and  $p_2$  and of  $\text{Re}(z_{1,2})$  were taken from the third column of Table 6 and used as the basis for a new design. The new design requirements, element values, and open-loop and closed-loop responses are given in Table 11. It can be seen that while the closed-loop response is improved, bandwidth sensitivity is still extremely large.

Eqs. 130 and 131 must be modified slightly to include contributions to sensitivity from non-dominant poles and zeros which are uncompensated. This results in the addition of terms of the form

$$\begin{aligned}
 & - \frac{|q_1| \left| \left| \frac{s^{q_1}}{s_{T_0}} \right| \right|}{\text{Im}(q_1)} \text{Im} \left[ \sum_r \frac{1}{q_1 - p_r} \frac{s^{p_r}}{T} - \sum_s \frac{1}{q_1 - z_s} \frac{s^{z_s}}{T} \right] \\
 & \approx - |q_1| \left| \left| \frac{s^{q_1}}{s_{T_0}} \right| \right| \left[ \sum_r \frac{1}{p_r} \frac{s^{p_r}}{T} - \sum_s \frac{1}{z_s} \frac{s^{z_s}}{T} \right] \quad (132)
 \end{aligned}$$

and

$$\begin{aligned}
 & 2 Q \left| \left| \frac{s^{q_1}}{s_{T_0}} \right| \right| \text{Re} \left[ \sum_r \frac{1}{q_1 - p_r} \frac{s^{p_r}}{T} - \sum_s \frac{1}{q_1 - z_s} \frac{s^{z_s}}{T} \right] \\
 & \approx 2 Q \left| \left| \frac{s^{q_1}}{s_{T_0}} \right| \right| \left[ \sum_r \frac{1}{-p_r} \frac{s^{p_r}}{T} - \sum_s \frac{1}{-z_s} \frac{s^{z_s}}{T} \right] \quad (133)
 \end{aligned}$$

where  $p_r$  and  $z_s$  represent any real non-dominant open-loop poles and zeros and where it is assumed

Table 11

- Revised Design Requirements, Element Values, and Response for a Second-Order Optimization of the Gaash Realization. (Frequency in rad/sec x 10<sup>6</sup>. Sensitivity in ppm/°C.)

Revised Design Requirements			
$p_1$	= -0.0565	$q_{1,2}$	= -0.00500 ± j0.500
$p_2$	= -0.206	$\omega_0$	= 0.500
$p_3$	= -0.418	BW	= 0.0100
$z_{1,2}$	= -0.125 ± j0.723	Q	= 50.0
$T_0$	= 62.55	$\gamma_T^{T_0}$	= +4537

New Element Values			
$R_{E1}$	= 7.5 $\Omega$	$R_{BT}$	= 96.5 $\Omega$
$R_F$	= 4.1 k $\Omega$	$C_3$	= 804.0 pf.

Open-Loop Response			
$p_1$	= -0.0565	$\gamma_T^{p1}$	= -1730
$p_2$	= -0.206	$\gamma_T^{p2}$	= -1440
$p_3$	= -0.419	$\gamma_T^{p3}$	= -1380
Re ( $z_1$ )	= -0.125	$\gamma_T^{\text{Re}(z_1)}$	= -1193
Im ( $z_1$ )	= -0.716	$\gamma_T^{\text{Im}(z_1)}$	= -1193
$T_0$	= 61.1	$\gamma_T^{T_0}$	= +4390

Closed-Loop Response			
$\omega_0$	= 0.497	$\gamma_T^{\omega_0}$	= -208
BW	= 0.0955	$\gamma_T^{BW}$	= -7800
Q	= 52.1	$\gamma_T^Q$	= +7600

$$|p_r| \gg |q_1|$$

$$|z_s| \gg |q_1|$$

The only additional pole which need be considered for the case at hand is at  $-36.5 \times 10^6$  rad/sec and has a temperature sensitivity of  $-4060$  ppm/ $^{\circ}$ C. It is due largely to  $c_{\pi 1}$  ( $\approx 20.2$  pf.) as can be demonstrated by the fact that upon removal of  $c_{\pi 1}$  from the circuit, the nearest pole is at  $-91.3 \times 10^6$  rad/sec. All other non-dominant open-loop poles and zeros are an additional two orders of magnitude removed from frequencies of interest ( $\approx |q_1|$ ), and from the form of Eqs. 132 and 133, it is easily seen that their contributions will be negligible. Then for

$$\Delta s_T^{p_1} \approx -0.162$$

$$\Delta s_T^{p_2} \approx -0.075$$

$$\Delta s_T^{p_3} \approx -0.054$$

$$\Delta s_T^{p_{\pi 1}} \approx -1.22$$

one obtains



$$S_T^{\omega_0} \approx -(0.133) \left[ \text{Im} \left( \frac{-0.162}{q_1-p_1} + \frac{-0.075}{q_1-p_2} + \frac{-0.054}{q_1-p_3} \right) + \frac{0.5}{-36.5} (-1.22) \right]$$

$$\approx -(0.0432 + 0.0171 + 0.0078 + 0.0022)$$

$$\approx -0.0703$$

$$S_T^{\text{BW}} \approx 2(50)(0.133) \left[ \text{Re} \left( \frac{-0.162}{q_1-p_1} + \frac{-0.075}{q_1-p_2} + \frac{-0.054}{q_1-p_3} \right) + \frac{-1.22}{36.5} \right]$$

$$\approx -(0.445 + 0.671 + 0.796 + 0.445)$$

$$\approx -2.26$$

or at 300°K

$$\gamma_T^{\omega_0} \approx -236 \text{ ppm}/^\circ\text{C}$$

$$\gamma_T^{\text{BW}} \approx -7520 \text{ ppm}/^\circ\text{C}$$

Again it is seen that these values agree reasonably well with the sensitivities of center frequency and bandwidth observed in Table 11.

~~An interesting point to notice is the comparatively low~~ sensitivity of bandwidth observed in Table 10 to that seen in Table 11. The failure of the preceding analysis to reflect this result is due to the fact that to first-order, compensation is not achieved for the second-order response

of Table 10 and Eq. 123 does not hold. The reduced bandwidth sensitivity seen in Table 10 is not due to the realization of required design values but to compensating errors in the realization of required design values. This phenomenon was observed several times during the course of preparing this report; however, all attempts to optimize in this direction failed.

By way of concluding this discussion then, the significant feature of the above analysis is the dependence of bandwidth sensitivity on the factor  $2Q$ . This causes what at first appear to be second-order perturbations from design requirements to have major effects on the observed sensitivities of bandwidth and selectivity with respect to temperature.

Before going on to consider ways in which the effects discussed above can be minimized, recall the following. It was assumed by Gaash that  $S_{T}^{R} = 0.36$  while a more reasonable value might be 0.6. For this larger value, however, the required loop gain sensitivity for the design proposed in Table 5 becomes  $S_{T}^{T0} \approx 2.25$  or  $\gamma_{T}^{T0} \approx 7500$  ppm/°C at 300°K. From the results of Section I.C, it is apparent that such a large value is incompatible with the circuit realization of Fig. 16. It then seems desirable to consider circuit modifications which both minimize loading effects and are compatible with a resistive temperature coefficient of 2000 ppm/°C.

↓ new design

Consider the selection of  $p_1$  and  $p_2$ . Momentarily ignoring the loading problem and using the previously outlined design procedure of Table 4, one can plot the curves of Fig. 18. The open-loop poles  $p_1$ ,  $p_2$ , and  $p_3$  were normalized to the center frequency  $\omega_0$  which was assumed to be 1.0. The selectivity was assumed to be 50. Here  $|p_2|$  was assumed to be the independent variable and  $|p_1|$  was then constrained such that the two innermost poles (the two poles nearest the origin) were coincident. Thus, for  $|p_2| > 0.4$ ,  $p_1 \approx p_3$ , and for  $|p_2| < 0.4$ ,  $p_1 \approx p_2$ . Empirically it was found that such a constraint assured a near minimal value for the required loop gain  $T_0$  for a particular choice of  $|p_2|$ . The required value of gain sensitivity was found to be almost entirely dependent on the value of the outermost pole. These curves give a fair indication of the types of design requirements which are likely to be encountered.

In choosing values for  $p_1$  and  $p_2$ , it will be helpful to keep in mind the following considerations. From the discussion of the second-order analysis of the optimized Gaash realization, it is apparent that excess phase due to non-dominant singularities can affect the sensitivity of the closed-loop response. It thus seems wise to use as few active devices as possible to minimize excess phase. This implies the use of a single inverting (common emitter) stage if one wishes to use negative feedback. The restriction to a single inverting stage, however, places severe limits on

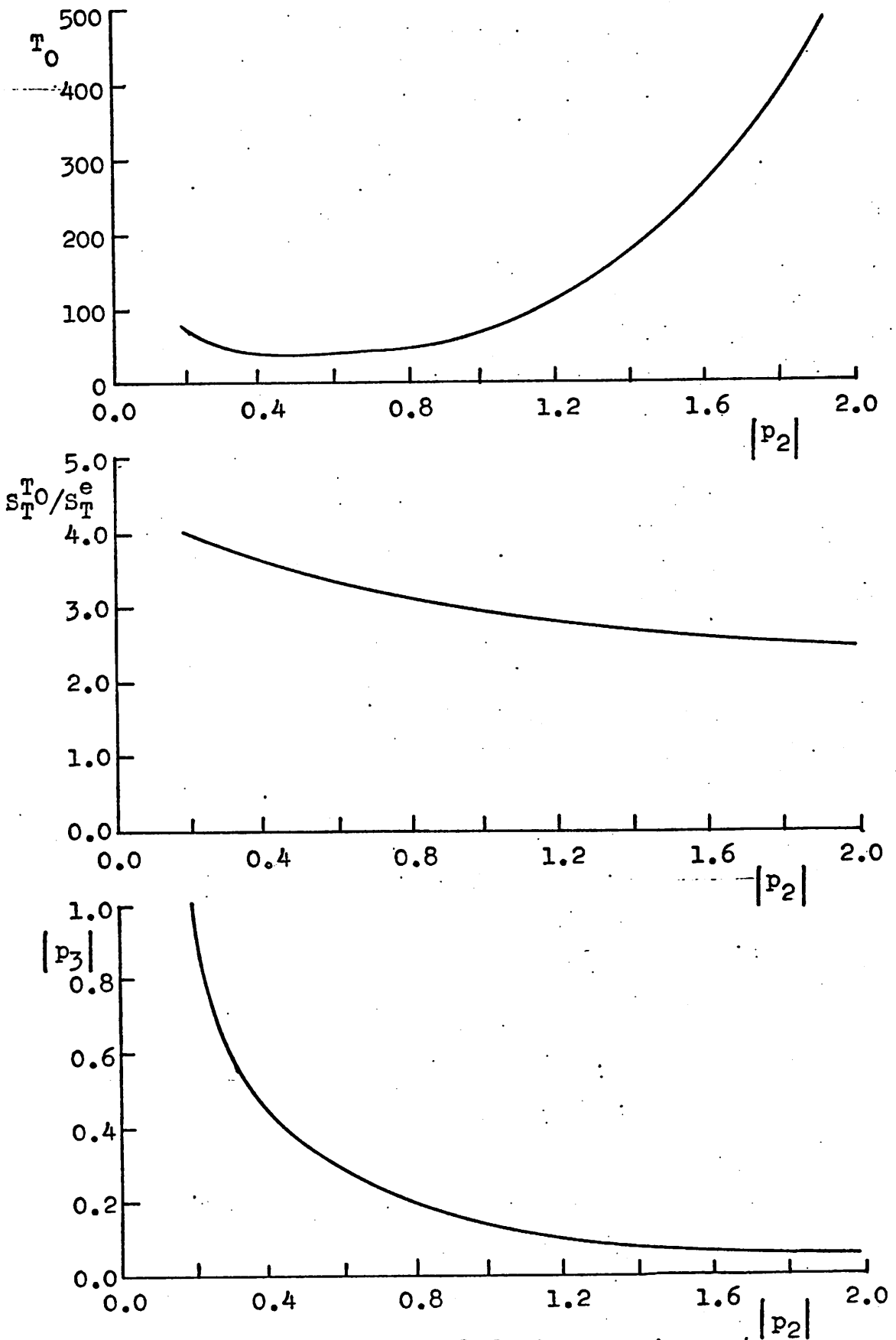


Fig. 18. Summary of typical design requirements.

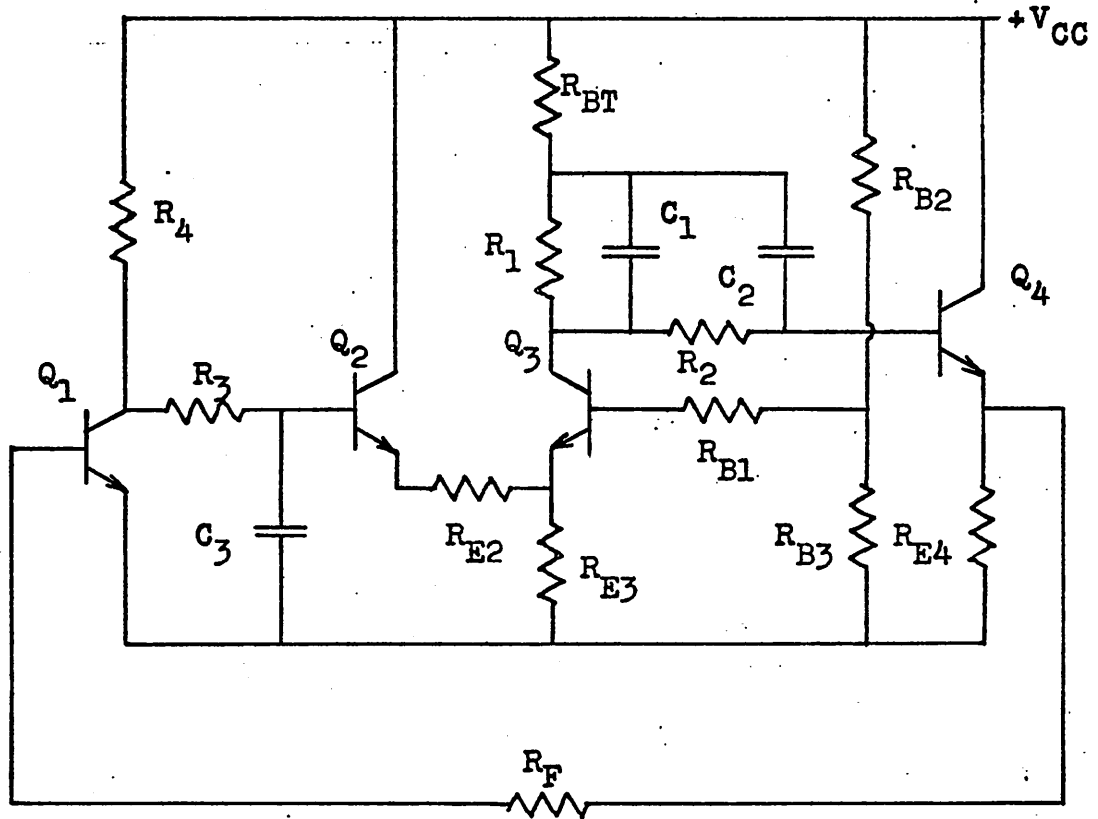
the amount of loop gain and loop gain sensitivity which can reasonably be realized.

If emitter followers are to be used in the manner employed by Gaash to achieve isolation, it would seem wise in view of earlier observations to make  $|p_1|$ ,  $|p_2|$ , and  $|p_3|$  as small as possible with respect to  $|q_1|$  in anticipation of effects of active loading on sensitivity. Unfortunately, this demand is not compatible with the constraint employed in generating the curves of Fig. 18. Further, it does not work out well in practice as the phase conditions upon which the design procedure is based severely limit the degree to which the magnitudes of the three open-loop poles can be minimized simultaneously.

As a compromise, consider a choice of  $|p_2|$  near  $1.4\omega_0$  and  $|p_1| \approx |p_3|$  near  $0.1\omega_0$ . This selection is prompted by the observation that as  $p_2$  is made increasingly large with respect to  $p_1$  its sensitivity more closely approaches the ideal value of  $-S \frac{R}{T}$ . Thus it would seem that contributions from both  $p_1$  and  $p_2$  can be minimized to some extent. From Fig. 18, this choice of  $p_1$  and  $p_2$  imply the need for a loop gain near 200 and a loop gain sensitivity near 1.65 (5500 ppm/°C at 300°K). An obvious solution based on the results of Section I.C is the addition of a common-base stage to the Gaash realization. This can be done with an unbalanced differential pair connected in the form of a paraphase circuit, though the inductive driving point impedance associated with

the common-base stage may lead to problems. Biasing considerations suggest the realization of Fig. 19.

Here it has been attempted to minimize the effects of loading by choosing relatively low values for resistances used in realizing the dominant open-loop poles and zeros where possible and large emitter resistors at each of the emitter-followers. The bridged-T network has been moved to take advantage of the larger driving point impedance obtained at the base of the second emitter-follower. Based on values required for biasing, a first-order analysis was performed to assess the range of loop gains and gain sensitivities available by varying  $R_F$  about a nominal value of  $5\text{ k}\Omega$ . Gain levels ranged from 204 at  $5\text{ k}\Omega$  to 299 at  $2.5\text{ k}\Omega$  while gain sensitivities ran from  $5410\text{ ppm}/^\circ\text{C}$  to  $4250\text{ ppm}/^\circ\text{C}$  at corresponding values of  $R_F$ . With these values in mind, the design procedure of Table 4 was used to seek a compatible set of design requirements while maintaining as small values for  $|p_1|$  and  $|p_3|$  as possible. This led to the design values shown in the first column of Table 12.  $C_1$  and  $C_2$  were then chosen so as to realize as closely as possible the required values of  $p_1$  and  $p_2$ . The actual values realized and the value of  $\text{Re}(z_{1,2})$  were then used as the basis for a new design, the results of which are presented in the second column of Table 12 for comparison.  $R_{BT}$ ,  $R_F$ , and  $C_3$  were then chosen so as to closely approximate the remaining design values.



$R_1 = 10 \text{ k}\Omega$	$R_{BT} = 281 \Omega$	$R_F = 4.3 \text{ k}\Omega$
$C_1 = 452 \text{ pF}$	$R_{E2} = 2 \text{ k}\Omega$	$V_{CC} = 6.5 \text{ V}$
$R_2 = 5 \text{ k}\Omega$	$R_{E3} = 500 \Omega$	$I_{C1} = 1.0 \text{ mA}$
$C_2 = 1505 \text{ pF}$	$R_{E4} = 10 \text{ k}\Omega$	$I_{C2} = 0.2 \text{ mA}$
$R_3 = 5 \text{ k}\Omega$	$R_{B1} = 10 \text{ k}\Omega$	$I_{C3} = 0.5 \text{ mA}$
$R_4 = 5 \text{ k}\Omega$	$R_{B2} = 10 \text{ k}\Omega$	$I_{C4} = 0.1 \text{ mA}$
$C_3 = 2616 \text{ pF}$	$R_{B3} = 2 \text{ k}\Omega$	

Fig. 19. Selective amplifier realization with paraphase interstage.

Table 12

Initial and Final Proposed Design Requirements  
 for the Selective Amplifier Realization of Fig. 19.  
 (Frequency in rad/sec x 10<sup>6</sup>. Sensitivity in ppm/°C.)

	Initial Values	Final Values
$q_{1,2}$	$-0.00500 \pm j0.500$	$-0.00500 \pm j0.500$
$\omega_0$	0.500	0.500
BW	0.0100	0.0100
Q	50.0	50.0
$p_1$	-0.0400	-0.0399
$p_2$	-0.7575	-0.7580
$p_3$	-0.0400	-0.0401
$z_{1,2}$	$-0.3987 \pm j0.9576$	$-0.3983 \pm j0.9577$
$-\gamma_T^e$	-2000	-2000
$T_0$	220.8	221.0
$\gamma_T^{T_0}$	+5210	+5211



The results of a first-order analysis are presented in the first column of Table 13. Again the deviations from the assumed values of temperature sensitivity of the open-loop poles  $p_1$  and  $p_3$  are noticeable. An analysis such as that previously performed on the Gaash realization based on Eqs. 130 and 131 yields the following

$$S_T^{\omega_0} \approx -(0.0286 + 0.0286) \approx -0.0572$$

$$S_T^{BW} \approx -(0.194 + 0.194) \approx -0.388$$

At 300°K

$$\gamma_T^{\omega_0} \approx -191 \text{ ppm/}^\circ\text{C}$$

$$\gamma_T^{BW} \approx -1290 \text{ ppm/}^\circ\text{C.}$$

where it has been assumed

$$\left| S_T^{q_1} \right| \approx |q_1| \left( \left| S_T^R / S_T^{T_0} \right| \right) \approx 0.192$$

Note that to first-order at least, the sensitivity and response obtained above is superior to that obtained from a first-order analysis of the optimized Gaash realization.

Finally, consider the results of the second-order analysis as presented in the second column of Table 13. While the open-loop results are not unexpected, the closed-loop poles

Table 13

Response and Response Sensitivity for the Selective Amplifier Realization of Fig. 19. (Frequency in rad/sec x 10<sup>6</sup>. Sensitivity in ppm/°C.)

Open Loop	First-Order	Second-Order
$p_1$	-0.0399	-0.0421
$\gamma_T^{p_1}$	-2240	-2350
$p_2$	-0.0401	-0.0437
$\gamma_T^{p_2}$	-2240	-2560
$p_3$	-0.7580	-0.7447
$\gamma_T^{p_3}$	-1980	-2130
$z_{1,2}$	$-0.3983 \pm j0.9576$	$-0.3983 \pm j0.9576$
$\gamma_T^{\text{Re}(z_1)}$	-1980	-1980
$\gamma_T^{\text{Im}(z_1)}$	-1980	-1980
$T_0$	220.8	156.8
$\gamma_T^{T_0}$	+5170	+5380

Closed Loop	First-Order	Second-Order
$q_{1,2}$	$-0.00502 \pm j0.500$	$+0.00921 \pm j0.463$
$q_3$	-1.077	-1.070
$z_{1,2}$	$-0.4469 \pm j0.9320$	$-0.4469 \pm j0.9320$
$\omega_0$	0.500	-----
$\gamma_T^{\omega_0}$	-228	-----
BW	0.0100	-----
$\gamma_T^{\text{BW}}$	-1470	-----
Q	50.0	-----
$\gamma_T^Q$	+1240	-----

$q_{1,2}$  migration into the right-half plane was not anticipated. This shift results from an additional open-loop pole at  $-6.04 \times 10^6$  rad/sec. As has been noted by others<sup>21</sup>, this narrowbanding is characteristic of the paraphase interstage. The inductive driving point impedance of the common base transistor is augmented by the emitter follower. A root locus corresponding to the first-order (dashed curve) and to the second-order (solid curve) analyses is shown in Fig. 20 and was obtained from a computer analysis.

Though it might be possible by a design modification to realize the desired closed-loop response taking into account the additional open-loop pole, note the following. The additional pole has a temperature sensitivity of  $-5110$  ppm/ $^{\circ}$ C. Consider the contribution to bandwidth sensitivity from Eq. 133 where it is assumed  $S_{T_0}^{q_1} \approx 0.192$

$$S_T^{BW} \approx -4.88$$

$$\gamma_T^{BW} \approx -16260 \text{ ppm/ } ^{\circ}\text{C}$$

at  $300^{\circ}$ K. At this point, one is forced to abandon this particular realization.

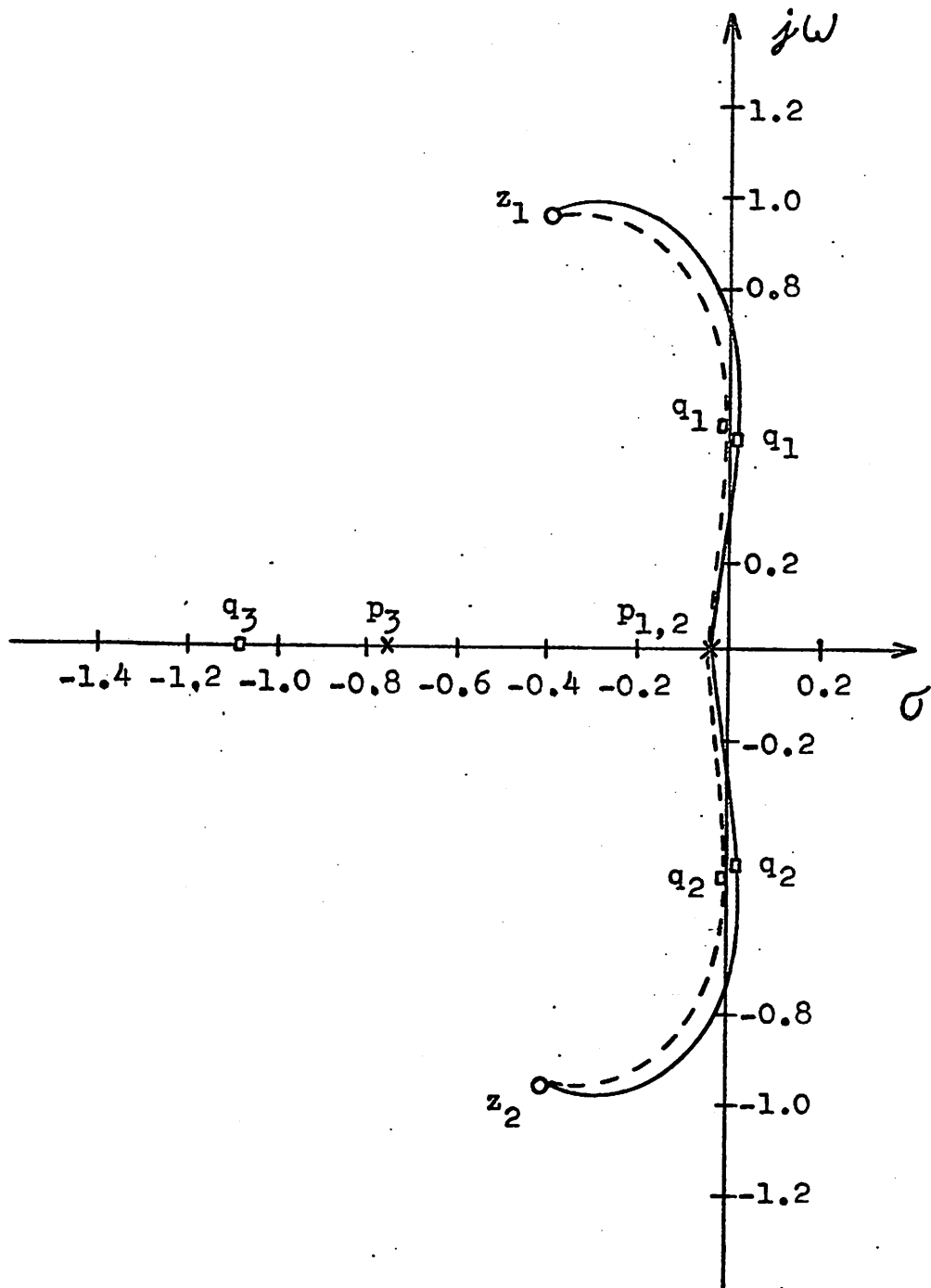


Fig. 20. Root locus for a first-order analysis of the selective amplifier of Fig. 19 (dashed curve) and the effects of excess phase for a second-order analysis (solid-curve).

## SUMMARY

An approach to the design of temperature insensitive, active RC selective amplifiers proposed by Gaash has been considered. Its development has been retraced using computer-aided analysis and simulation. Single-loop, negative feedback amplifier realizations were employed. First-order sensitivity formulations were used to relate the dependence of the required dominant complex pair of closed-loop poles on temperature to the behavior of the open-loop poles and zeros and the low frequency value of the loop transmission or loop gain function. It was shown that, to first-order, simplifications in the sensitivity expressions resulted when all open-loop poles and zeros were constrained to have the same temperature coefficient. These simplifications were shown by Gaash to lead to a simple physical description of the sensitivity of the closed-loop poles in the complex frequency plane. The need for extra degrees of freedom in the form of additional open-loop poles and zeros to be able to design for desired response and response invariance was demonstrated.

The single-loop realization proposed by Gaash was examined in detail with respect to the effects introduced by first and second-order device models. Charge storage (excess phase) in active devices, resistive losses, and non-ideal realization were considered. It was seen that

deviations in the temperature dependence of the open-loop poles and zeros from prescribed values had major effects on the observed sensitivities of bandwidth and selectivity with respect to temperature. In particular, bandwidth sensitivity was found to be proportional to  $2Q$ . Efforts to minimize these second-order effects while extending the design approach to accommodate a resistive temperature coefficient of 2000 ppm/°C led to unacceptable results.

The problem remains of reconciling the excellent experimental results reported by Gaash with the poor results reported here. Two possibilities seem to exist. The first is that non-linearities in device parameters or their temperature dependence inaccurately simulated on the computer had a compensating effect which has not been accounted for. The second is that variations in temperature coefficients of elements of the same type resulted in compensation. In this regard it can be demonstrated that had  $R_{BT}$  had a temperature coefficient 200ppm/°C greater than the uniform temperature coefficient assumed by Gaash, much improved results would have been observed. Without knowing the geometry of the diffused resistors used by Gaash, it is not possible to say whether or not this could have occurred. It is known that Gaash worked with at least one experimental circuit in which discrete components were used. A comparison of the temperature coefficients of several commercially available 1% resistors indicated slight uniformity between units of the same

value from the same manufacturer while units of different values showed no correlation at all. The main conclusion seems to be then that while temperature compensation may occur when the approach considered by Gaash is used, the result cannot be considered to follow from the first-order design formulations presented.

Finally, a word should be said about the approach used in this report. In defense of computer-aided analysis and simulation it must be said that no other method of analysis seems possible. However, computer-aided analysis and simulation cannot be considered a substitute for intelligent consideration and understanding of underlying physical processes. As the author began spending what seemed like an inordinate amount of time verifying computer results, finding that sometimes mistakes were made by the computer, more often by the program, and most often by himself, it became abundantly clear that no computer result should ever be accepted uncritically. Therefore, it is the author's contention that this report should not be considered grounds for dismissal of Gaash's work but as an additional piece of information bearing on an imaginative approach to the design of temperature insensitive selective amplifiers.

## REFERENCES

1. D. F. Sheahan and H. J. Orchard, "Bandpass-Filter Realization using Gytrators," *Electronics Letters*, Vol. 3, No. 1, Jan. 1967.
2. R. W. Newcomb, T. N. Rao, and J. Woodard, "A Minimal Capacitor Cascade Synthesis for Integrated Circuits," *Microelectronics and Reliability*, Vol. 6, No. 2, May 1967.
3. J. G. Linvill, "RC Active Filters," *Proc. IRE*, Vol. 42, March 1954.
4. T. Yanagisawa, "RC Active Networks using a Current Inversion Type Negative Impedance Converter," *IRE Trans. CT*, CT-4, No. 3, Sept. 1957.
5. I. M. Horowitz, "Optimization of Negative Impedance Converter Methods of Active RC Synthesis," *IRE Trans. CT*, CT-6, No. 3, Sept. 1959.
6. G. A. Rigby and D. G. Lampard, "Integrated Selective Amplifiers for RF," *Digest of Technical Papers, 1968 International Solid State Circuits Conference*, Vol. XI, Feb. 1968.
7. A. A. Gaash, "Synthesis of Integrated Selective Amplifiers for Specified Response and Desensitivity," *ERL Report No. 65-31, University of California, Berkeley*, June 1965.
8. A. A. Gaash, R. S. Pepper, and D. O. Pederson, "Design of Integrable Desensitized Frequency Selective Amplifiers," *IEEE J. on Solid State Circuits*, Vol. SC-1, No. 1, Sept. 1966.
9. D. A. Calahan, "Linear Network Analysis and Realization Digital Computer Programs: An Instruction Manual," *University of Illinois Bulletin*, Vol. 62, No. 58, Feb. 1965.
10. C. Pottle, "Comprehensive Active Network Analysis by Digital Computer--A State Space Approach," *Proc. Third Allerton Conf., Urbana, Ill., October 1965*.
11. W. M. Syn, "BEV4--A Transfer Function Linear Analysis Program," *IBM Technical Rept. TR 02.339, San Jose*, Dec. 1964.



## APPENDIX A

### SENSITIVITY OF CLOSED-LOOP POLES IN SINGLE-LOOP FEEDBACK

Assume that the closed-loop transfer function  $A(s)$  of a single-loop feedback system is written in the form

$$A(s) = \frac{N(s)}{D(s)} = \frac{N(s)}{1 + T(s)} \quad (\text{A.1})$$

where  $D(s)$  (not necessarily a polynomial) is the return difference and  $T(s)$  is the loop transmission.  $T(s)$  may be written in one of the two forms

$$T(s) = T_0 \frac{\prod_k (1 - s/z_k)}{\prod_e (1 - s/p_e)} \quad (\text{A.2})$$

$$= K \frac{\prod_k (s - z_k)}{\prod_e (s - p_e)} \quad (\text{A.3})$$

where the low frequency value of the loop transmission,  $T_0$ , is given by

$$T_0 = T(0) \quad (\text{A.4})$$

and

$$K = T(0) \frac{\prod_e (-p_e)}{\prod_k (-z_k)} \quad (\text{A.5})$$

The return difference may be written in the form

$$D(s) = 1 + T(s) = \frac{\prod_e (s - p_e) + K \prod_k (s - z_k)}{\prod_e (s - p_e)} \quad (\text{A.6})$$

Let  $q_i$  ( $i = 1, 2, \dots, n$ ) denote the zeros of the return difference

$$D(s) = 1 + T(s) = \frac{\prod_i (s - q_i)}{\prod_e (s - p_e)} \quad (\text{A.7})$$

and equivalently the poles of the closed-loop transfer function  $A(s)$ .

Let  $q_1$  denote the closed-loop pole of interest. Evaluating  $D(s)$  at  $q_1$ , one obtains

$$D(s) \Big|_{s=q_1} = 1 + T(s) \Big|_{s=q_1} = \frac{\prod_i (s - q_i)}{\prod_e (s - p_e)} \Big|_{s=q_1} = 0 \quad (\text{A.8})$$

From Eq. A.6, the total differential of  $T(s)$  is given by

$$\begin{aligned} dT(s) &= dD(s) \\ &= \frac{\prod_e (s - p_e) d\prod_i (s - q_i) - \prod_i (s - q_i) d\prod_e (s - p_e)}{\prod_e (s - p_e)^2} \quad (\text{A.9}) \end{aligned}$$

and from Eq. A.8

$$dT(s) \Big|_{s=q_1} = \frac{d\prod_i (s - q_i)}{\prod_e (s - p_e)} \Big|_{s=q_1}$$

$$\begin{aligned}
&= \frac{\sum_{j \neq i}^n \prod (s-q_j) ds - \sum_{j \neq i}^n \prod (s-q_j) dq_1}{\prod_e (s-p_e)} \Big|_{s=q_1} \\
&= \frac{\prod_{j=2}^n (q_1-q_j) dq_1 - \prod_{j=2}^n (q_1-q_j) dq_1}{\prod_e (q_1-p_e)} \\
&= 0 \qquad \qquad \qquad (A.10)
\end{aligned}$$

From Eq. A.2 and Eq. A.7, it is apparent that a closed-loop pole, such as  $q_1$ , may be expressed as a function of  $T_0$ ,  $z_k$ , and  $p_e$ ; that is,

$$q_1 = q_1(T_0, z_k, p_e) \qquad (A.11)$$

where  $k=1, \dots, m$  and  $e=1, \dots, n$ . Consider the total differential of  $q_1$

$$\begin{aligned}
dq_1 &= \frac{\partial q_1}{\partial T_0} dT_0 + \sum_k \frac{\partial q_1}{\partial z_k} dz_k + \sum_e \frac{\partial q_1}{\partial p_e} dp_e \\
&= T_0 \frac{\partial q_1}{\partial T_0} \frac{dT_0}{T_0} + \sum_k z_k \frac{\partial q_1}{\partial z_k} \frac{dz_k}{z_k} + \sum_e p_e \frac{\partial q_1}{\partial p_e} \frac{dp_e}{p_e} \\
&= s_{T_0}^{q_1} \frac{dT_0}{T_0} + \sum_k s_{z_k}^{q_1} \frac{dz_k}{z_k} + \sum_e s_{p_e}^{q_1} \frac{dp_e}{p_e} \qquad (A.12)
\end{aligned}$$

where

$$s_{T_0}^{q_1} = T_0 \frac{\partial q_1}{\partial T_0} \qquad (A.13a)$$

$$s \frac{\partial q_1}{\partial z_k} = z_k \frac{\partial q_1}{\partial z_k} \quad (\text{A.13b})$$

$$s \frac{\partial q_1}{\partial p_e} = p_e \frac{\partial q_1}{\partial p_e} \quad (\text{A.13c})$$

From Eq. A.2 it is also apparent that the loop transmission,  $T$ , may be expressed as a function of  $s$ ,  $T_0$ ,  $z_k$ , and  $p_e$

$$T = T(s, T_0, z_k, p_e) \quad (\text{A.14})$$

where  $k=1, \dots, m$  and  $e=1, \dots, n$ .

From Eq. A.10, the total differential of  $T$  evaluated at  $s = q_1$  is given by

$$\begin{aligned} \left. \frac{dT}{ds} \right|_{s=q_1} &= 0 \\ &= \left[ \frac{\partial T}{\partial s} ds + \frac{\partial T}{\partial T_0} dT_0 + \sum_k \frac{\partial T}{\partial z_k} dz_k + \sum_e \frac{\partial T}{\partial p_e} dp_e \right]_{s=q_1} \end{aligned} \quad (\text{A.15})$$

Thus

$$\left[ \frac{\partial T}{\partial s} ds \right]_{s=q_1} = \left[ T_0 \frac{\partial T}{\partial T_0} \frac{dT_0}{T_0} + \sum_k z_k \frac{\partial T}{\partial z_k} \frac{dz_k}{z_k} + \sum_e p_e \frac{\partial T}{\partial p_e} \frac{dp_e}{p_e} \right]_{s=q_1} \quad (\text{A.16})$$

The individual partial derivatives may be evaluated from Eq. A.2. The result may be written

$$-dq_1 = \left( \frac{\partial T}{\partial s} \Big|_{s=q_1} \right)^{-1} \left[ \frac{dT_0}{T_0} - \sum_k \frac{q_1}{q_1 - z_k} \frac{dz_k}{z_k} + \sum_e \frac{q_1}{q_1 - p_e} \frac{dz_k}{z_k} \right] \quad (\text{A.17})$$

Comparing Eq. A.17 with Eq. A.12, one can identify the sensitivity functions as follows

$$S_{T_0}^{q_1} = \left( \frac{\partial T}{\partial s} \Big|_{s=q_1} \right)^{-1} \quad (\text{A.18a})$$

$$S_{z_k}^{q_1} = - S_{T_0}^{q_1} \frac{1}{q_1 - z_k} \quad k=1, \dots, m \quad (\text{A.18b})$$

$$S_{p_e}^{q_1} = S_{T_0}^{q_1} \frac{1}{q_1 - p_e} \quad e=1, \dots, n \quad (\text{A.18c})$$

$S_{T_0}^{q_1}$  may be evaluated from either Eq. A.2 or Eq. A.3; however, Eq. A.3 is chosen for convenience

$$\begin{aligned} S_{T_0}^{q_1} &= \left( \frac{\partial T}{\partial s} \Big|_{s=q_1} \right)^{-1} \\ &= \left( \frac{\partial}{\partial s} \frac{K \prod_k (s - z_k)}{\prod_e (s - p_e)} \Big|_{s=q_1} \right)^{-1} \\ &= \left( \frac{K \frac{\partial}{\partial s} \prod_k (s - z_k) - T \frac{\partial}{\partial s} \prod_e (s - p_e)}{\prod_e (s - p_e)} \Big|_{s=q_1} \right)^{-1} \quad (\text{A.19}) \end{aligned}$$

$$= \frac{\pi_e(s - p_e)}{\frac{\partial}{\partial s} \prod_i (s - q_i)} \Big|_{s=q_1} \quad (\text{A.20})$$

$$= \text{Res}_{s=q_1} \frac{\pi_e(s - p_e)}{\prod_i (s - q_i)} \quad (\text{A.21})$$

$$= \frac{\pi_e(s - p_e)}{\prod_{j=2}^n (s - q_j)} \Big|_{s=q_1} \quad (\text{A.22})$$

A second form can be obtained from Eq. A.19

$$S_{T_0}^{q_1} = \left( \frac{K \sum \pi(s - z_k)}{\pi(s - p_e)} - \frac{T(s) \sum \pi(s - p_e)}{\pi(s - p_e)} \right)_{s=q_1}^{-1}$$

$$= \left( \sum_e \frac{1}{q_1 - p_e} - \sum_k \frac{1}{q_1 - z_k} \right)^{-1} \quad (\text{A.23})$$